HHS Public Access

Author manuscript

Int J Hyperthermia. Author manuscript; available in PMC 2024 January 01.

Published in final edited form as:

Int J Hyperthermia. 2023 ; 40(1): 2233720. doi:10.1080/02656736.2023.2233720.

The histotripsy spectrum: differences and similarities in techniques and instrumentation

Randall P. Williams[1,2], **Julianna C. Simon**[3], **Vera A. Khokhlova**[2,4], **Oleg A. Sapozhnikov**[2,4], **Tatiana D. Khokhlova**[1,2]

[1]Department of Medicine, University of Washington Medical Center, 1959 NE Pacific Street, Box 356510, Seattle, WA 98195, USA

[2]Center for Industrial and Medical Ultrasound, Applied Physics Laboratory, University of Washington, 1013 NE 40th Street, Seattle, WA 98105, USA

[3]Graduate Program in Acoustics, The Pennsylvania State University, University Park, PA, 16802, USA

[4]Department of Acoustics, Physics Faculty, Moscow State University, Moscow 119991, Russia

Abstract

Since its inception about two decades ago, histotripsy – a non-thermal mechanical tissue ablation technique – has evolved into a spectrum of methods, each with distinct potentiating physical mechanisms: intrinsic threshold histotripsy, shock-scattering histotripsy, hybrid histotripsy, and boiling histotripsy. All methods utilize short, high amplitude pulses of focused ultrasound delivered at low duty cycle, and all involve excitation of violent bubble activity and acoustic streaming at the focus to fractionate tissue down to subcellular level. The main differences are in pulse duration, which spans microseconds to milliseconds, and ultrasound waveform shape and corresponding peak acoustic pressures required to achieve the desired type of bubble activity. In addition, most types of histotripsy rely on the presence of high-amplitude shocks that develop in the pressure profile at the focus due to nonlinear propagation effects. Those requirements, in turn, dictate aspects of the instrument design, both in terms of driving electronics, transducer dimensions and intensity limitations at surface, shape (primarily, the *F*-number) and frequency. The combination of the optimized instrumentation and the bio-effects from bubble activity and streaming on different tissues, lead to target clinical applications for each histotripsy method. Here, the differences and similarities in the physical mechanisms and resulting bioeffects of each method are reviewed and tied to optimal instrumentation and clinical applications.

Keywords

high intensity focused ultrasound; nonlinear propagation; histotripsy; boiling histotripsy; cavitation

Vera Khokhlova verak2@uw.edu.

DISCLOSURE STATEMENT

Dr. Tatiana Khokhlova has a financial interest in *Petal Surgical Inc.*

1. INTRODUCTION

Histotripsy is a pulsed high intensity focused ultrasound (HIFU) method that is mediated by bubble activity and leads to mechanical disintegration of tissue or other material, such as blood clots, large hematomas, or abscesses, at the focus down to subcellular level. The term histotripsy (from *histo* – soft tissue and *tripsis* – to break) was coined at the University of Michigan where the technique was first demonstrated [1-3]. Over two decades, the field of histotripsy has dramatically progressed and expanded to include a variety of distinct techniques illustrated in Fig.1. All techniques have the same ultimate effect of tissue liquefaction, and all use very short (microseconds to milliseconds) HIFU pulses delivered at low (typically under 2-3%) duty cycle to avoid heat accumulation and thermal damage. The differences are in the specifics of bubble nucleation and dynamics and therefore in the pulse durations, acoustic pressure levels, degrees of nonlinear waveform distortion, and aspects of transducer design and driving electronics, which are required to achieve specific histotripsy conditions. The purpose of this review is to highlight the distinctive features of each technique and ways in which those features are enabling certain applications of histotripsy. As such, it is by no means an exhaustive review on any one technique or applications thereof; for that, please see prior reviews on the subject [4, 5].

This review is also limited to “endogenous” histotripsy, i.e. without the use of any extraneously administered ultrasound contrast agents or cavitation nuclei such as nanodroplets, nanoparticles, and microbubbles [6-8]. The field of contrast-enhanced histotripsy has dramatically expanded recently, and its thorough analysis would be impossible within the confines of the current review.

Historically, shock-scattering histotripsy was the first technique to be discovered; its feasibility has been shown in *ex vivo* tissues and *in vivo*, and the underlying bubble dynamics have been investigated [2, 3, 9]. Shock-scattering histotripsy uses bursts of HIFU consisting of 3-20 cycles at the peak output powers sufficient for attaining high-amplitude shock fronts at the focus and peak negative pressures of approximately 20-25 MPa. Within each burst, a dense cloud of bubbles a few millimeters in size is formed [9]. The subsequent violent collapse of bubbles in this cloud imposes high transient shear strain and stress on the adjacent cells and tissue structures and leads to their rupture. Accumulation of this damage over multiple collapses ultimately leads to disintegration of tissue down to the level of peptide slurry within the focal region of the beam.

Boiling histotripsy was first reported in 2009 [10, 11], and termed as such in 2014 [12]. Boiling histotripsy uses longer – 1-20 milliseconds - bursts of HIFU, at lower peak output powers compared to shock-scattering histotripsy, but sufficient to reach the formation of shock fronts with >40 MPa amplitude at the focus. Enhanced heat deposition through absorption at the shocks leads to rapid elevation of temperature up to 100°C in a very localized volume at the focus within a few milliseconds, which in turn leads to the generation of a vapor bubble [13]. The interaction of this vapor bubble with the remaining cycles of the burst leads to tissue fractionation through a number of physical mechanisms [11, 14-16]. The peak negative focal pressure used in boiling histotripsy is within 9-19 MPa,

and is ideally kept low to avoid initiating prefocal cavitation that can shield the focus from shock waves [17].

Intrinsic threshold histotripsy was first reported in 2014 [18] and was originally termed microtripsy due to the emphasis on producing small, sub ultrasound wavelength bubble clouds and corresponding lesions. In subsequent works, this regime was optimized for ablation of larger volumes using higher pressures and lower frequencies [19, 20], thus the "intrinsic threshold" or "homogenous nucleation" terminology appeared more appropriate. This regime uses extremely short HIFU pulses, < 2 cycles and ideally as close to only one rarefaction half-cycle as possible, with very high peak negative pressure that exceeds the threshold for the formation and explosive growth of bubbles from nano-scale nuclei that are intrinsic to a medium. In water-based tissues this threshold is within 25-30 MPa range [21], and a cavitation cloud forms only within the focal region where cavitation threshold is exceeded. While tissues are inherently heterogenous, the study of spontaneous nucleation was first investigated in homogeneous media, and, as a result, the process has also become known as homogeneous nucleation [22]. Both shock-scattering histotripsy and intrinsic threshold histotripsy are together often referred to as "cavitation cloud histotripsy" in the literature. Keeping peak compressional pressures low and avoiding the formation of shock fronts are preferred in this histotripsy regime to maximize the large tensile pressure phase at the focus.

The most recent regime of histotripsy, first reported in 2016 [23, 24], uses pulse durations of hundreds of microseconds and acoustic output levels in between shock-scattering and boiling histotripsy. This regime has been termed as "hybrid histotripsy" [25]. The HIFU focal waveforms used in those studies contained shock fronts that were insufficient to achieve boiling temperature within a single pulse, but were confirmed to lead to moderate tissue temperature increase, which was hypothesized to promote the nucleation and growth of cavitation bubbles that ultimately potentiated the formation of clouds. Furthermore, due to gradual heat accumulation over multiple pulses, the formation of vapor bubbles could be also achieved after a few seconds of exposure and contribute to tissue fractionation.

It is important to mention here that while histotripsy techniques have been termed as such and developed fairly recently, tissue fractionation using similar pulsed HIFU regimes has been reported on previously but were not termed histotripsy. One of the first examples of histotripsy dates back to 1994 [26], where rabbit liver tissue was fractionated (although not completely) by cavitation induced by short high-amplitude shock waves resembling a cross between intrinsic threshold and shock-scattering histotripsy. In another study, 40 ms HIFU pulses with shock fronts were used to liquefy subcutaneously grafted MC-38 colon adenocarcinoma tumors in mice and trigger systemic anti-tumor immune response [27]; this regime was termed M-HIFU and most likely represented a variation of boiling histotripsy.

As mentioned above, complete tissue fractionation without discernable thermal effects is similar across the histotripsy spectrum, as long as the time-averaged acoustic power deposited into tissue – a combination of peak power and duty cycle - remains under certain limits. If those limits are exceeded, the viscous heating associated with large velocity gradients of the tissue involved in rapid movement during bubble collapses and HIFU

absorption by prefocal tissue cannot be compensated by heat diffusion and lead to heat accumulation inside and around the lesion [11, 28, 29]. This heat buildup leads, first, to the contents of the lesion being partially denatured and becoming “paste-like”, and the rim of the lesion becoming heat-fixed – at its extreme, the lesion becomes completely solid and denatured, with large vacuoles [1, 28, 30, 31]. While thermal effects are typically avoided in histotripsy, mild temperature elevations may potentially be beneficial in certain applications involving, for example, breakdown of tissues high in collagen [32], where mild heat or mild hyperthermia softens adjacent tissues to stimulate immune responses.

An important aspect of the bioeffects induced by histotripsy is differential sensitivity of tissues to histotripsy-mediated destruction: connective tissue structures and tissues high in collagen and elastin are more resistant to fractionation than cells [32-37]. This is beneficial in applications where sparing of critical structures – blood vessels, nerves, ducts, organ capsules – adjacent to or present inside of the region to be ablated is important. However, this is a challenge in applications where the tough, fibrous tissue, e.g. ligaments, cartilage or fibrous tumors like uterine fibroids or benign prostate hyperplasia, is itself the target of intervention. Some histotripsy pulsing parameters, sometimes even within the same histotripsy technique, were shown to be more efficient at liquefying such tissues than others, which will be reviewed in more detail in corresponding sections below.

2. PHYSICAL MECHANISMS POTENTIATING HISTOTRIPSY METHODS

Representative focal pressure waveforms, axial beam profiles, and schematic illustrations of the bubble clouds are shown in Figure 2 for intrinsic threshold histotripsy, shock scattering histotripsy, and boiling histotripsy. Differences between the methods, along with hybrid histotripsy, are presented in the following sections.

2.1 Intrinsic threshold histotripsy

In intrinsic threshold histotripsy, bubbles form and grow explosively in target medium when the peak negative pressure (p_-) in the tensile phase of the very short (<=2 cycles) HIFU pulse exceeds a value termed “intrinsic threshold”, as illustrated Fig. 2(a). The intrinsic threshold predicted for pure water based on classical nucleation theory is greater than 130 MPa [38, 39], much higher than p_- achievable in therapeutic ultrasound. However, the presence of intrinsic cavitation nuclei – ubiquitous nano- and sub-nanoscale inhomogeneities which may always be expected to be present in a medium – reduces the threshold by an order of magnitude. While it would be reasonable to expect that a perfectly pure liquid would contain no such nuclei, a wealth of experimental evidence and modeling suggest that ion-stabilized bubbles, thermodynamic fluctuations of the equilibrium state, or even cosmic rays [22, 40] can create nuclei which can serve to induce cavitation when stimulated. Experiments attempting to remove intrinsic nuclei from water by multiple purifications have not been successful [40-42], supporting the idea that they are indeed intrinsic to the medium.

Cavitation is a stochastic process, meaning that the formation of a cavitation bubble in response to an applied acoustic pulse is associated with a finite probability. Accordingly, the intrinsic cavitation threshold was defined as the value of p_- above which the probability of generating a cavitation bubble cloud exceeds 50% in response to a pulse with a single

dominant tensile phase. Measured values of the intrinsic threshold in filtered, degassed water range from about 25 to 28 MPa [21, 43], which agree with reported cavitation thresholds measured in water by non-acoustic means [41]. In water-based tissues, thresholds are between about 25 MPa and 30 MPa, and are largely insensitive to the ultrasound frequency within 345 kHz to 2 MHz range and tissue stiffness within 1.1 kPa to 570 kPa [21, 43, 44]. The thresholds are much lower for adipose tissues with values reported between 10 MPa and 17 MPa [21, 45]. Paradoxically, while adipose tissue comprises roughly 80% triglycerides, the intrinsic threshold for olive oil (nearly 100% triglycerides), is greater than 36 MPa, thus it was hypothesized that lipid/water interfaces abundant in adipose tissue are responsible for its lower intrinsic threshold [21]. Another tissue parameter that is known to decrease the intrinsic threshold is temperature: for instance, in water the threshold decreases from roughly 30 MPa at 10 °C to 15 MPa at 90 °C [46].

A bubble cloud formed by intrinsic threshold histotripsy is consistently localized to within the region of the HIFU beam where the intrinsic threshold is exceeded [18, 20], as illustrated in Figs. 2(b) and 2(c). Outside this region, no bubbles form, and the clouds induced in this manner do not migrate, providing for high spatial selectivity and ways to generate lesions as small as half of the −6 dB beamwidth of the transducer, and larger lesions – at higher output power [47]. This control of the bubble cloud also avoids any off-target damage by the side lobes, as long as p_- in the focal lobe is above the threshold and below it in the sidelobes. The length and width of the focal lobe are inversely proportional to the HIFU frequency and highly dependent on the focusing angle or *F*-number of the transducer, defined as the ratio of the focal distance to the width of the aperture. Observations of bubble clouds in water-based gel phantoms show that the intrinsic threshold is insensitive to the transducer *F*-number within 0.51-0.89 range but the density of the clouds is greatly reduced as the *F*-number increases, resulting in less effective fractionation [48]. This effect is attributed to a phenomenon known as bubble-induced pressure saturation – a temporary reduction in tensile pressure in the vicinity of a formed bubble causing p_- to drop below the intrinsic threshold for a short distance as the pulse propagates through the focal lobe [49]. More sharply focused transducers alleviate this issue, because they provide a higher spatial rate of pressure increase as the pulse propagates to the focus [48]. The second motivation for using strongly focused transducers is to avoid nonlinear propagation effects that distort HIFU pressure waveform in a way that reduces p_- and increases p_+. The degree of nonlinear distortion of ultrasound waveforms increases with both pressure amplitude and propagation length. In HIFU beams this distortion occurs primarily over the length of the focal lobe, thus the shorter it is (i.e. more focused transducers, lower *F*-number), the less pronounced nonlinear effects will be for a given focal p_- [50-52]. Furthermore, the focal gain of a transducer, defined as the ratio of peak focal pressure to that at the transducer surface, scales inversely with *F*-number, and thus using more focused transducers better facilitates achieving pressures exceeding the intrinsic threshold.

Apart from avoiding thermal effects, keeping pulse repetition frequency (PRF) low in intrinsic threshold histotripsy exposures is important for another reason: if the period between successive pulses is too short, the cavitation bubbles will not have time to fully dissolve back into the tissue and may re-occur in the same locations in subsequent pulses [53]. This effect is known as cavitation memory and can adversely impact the homogeneity

of the fractionated region. The amount of time required for the bubbles to fully dissolve back into the tissue depends on the characteristics of the bubbles and the properties of the medium. A recent study using agarose gel phantoms reported that as the PRF was increased from 1 Hz to 1 kHz, the bubble density was reduced and the locations of bubbles were more correlated from pulse to pulse [54]. While studies have shown that it can take up for 1 second for cavitation bubbles to completely dissolve in water-based tissues, [21, 43] using such a low PRF would result in excessively long treatment time. Solutions to this issue include consecutive electronic steering of the HIFU beam over a volume of locations to reduce the PRF encountered at each location [19] and low-amplitude pulses interspersed between histotripsy pulses to merge and dissolve the residual bubbles [55].

2.2 Shock-scattering histotripsy

Shock scattering histotripsy uses longer (3-20 cycles) pulses at a reduced p_- compared to intrinsic threshold regime, but containing high-amplitude shock fronts to generate large bubble clouds [9]. An example focal pressure waveform is shown in Fig. 2(d). The process of cloud formation involves so-called incidental bubbles [9, 43] that can form at p_- an order of magnitude smaller than the intrinsic threshold [56]. During the first 1-2 cycles of a shock-scattering histotripsy pulse, one or more such incidental bubbles are formed within the focal region. When the next shock front in the pulse arrives at the location of the incidental bubble, and if the bubble is large compared to the spatial thickness of the shock (*e.g.*, 100 μm *vs.* 70 nm in water [57]), its wall acts as a pressure-release surface for the incoming shock front and reflects it with inverted polarity. This inverted wave then adds constructively to the next tensional phase arriving from the transducer, and, if the net p_- exceeds the intrinsic threshold, more bubbles form proximally to the original bubble. These bubbles, in turn, serve as a pressure release surface for the next arriving shock front, and the bubble cloud continues to grow towards the HIFU source with each successive shock front, until it either reaches a point where the total p_- no longer exceeds the intrinsic threshold or the pulse ends. This process is schematically illustrated Fig. 2(e) and 2(f).

Thus, the shock-scattering mechanism allows for generation of a much larger bubble cloud, using lower pressures and less focused (higher *F*-number) transducers compared to intrinsic threshold histotripsy. On the other hand, the structure of the bubble cloud becomes more complex, and is dependent not only on the distribution of peak negative pressure, but also on HIFU frequency, number of excitation cycles, nonlinear asymmetry of the waveform, and the distribution of incidental nuclei in the medium. As a result, there is a greater variation between histotripsy initiation values reported in the literature; with the values of p_- ranging between 15 and 24 MPa in degassed water [41, 57], and between 13.5 MPa and 27 MPa for water-based tissues [21, 58]. In particular, the growth of the initial bubble from which the process of shock scattering begins is influenced by multiple factors. Unlike the intrinsic threshold, that is nearly independent of the HIFU frequency, the incidental threshold was found to decrease at lower frequencies [43, 47]. Longer pulses also increase the probability of incidental bubble formation through increasing the likelihood that a suitable nucleus will be located within the focal area, and that it will grow to a size sufficient for effective shock scattering through the process of rectified diffusion [59].

Multiple studies have examined the effect of tissue mechanical properties on the threshold for and damage induced by shock scattering histotripsy. A study by Vlaisavljevich *et al.* [58] investigated the threshold required to induce shock-scattering histotripsy in gel phantoms and *ex vivo* porcine tissues with different mechanical stiffnesses, quantified by the Young's modulus. It was seen that for tissues with stiffnesses below 25 kPa (lung, fat, kidney, liver, heart, muscle, and skin), the threshold was reduced along with the stiffness of the sample from 1.6 MPa to 25 MPa, while the threshold reached a plateau of 25 MPa to 30 MPa for tissues with Young's moduli at 25 kPa or higher – cartilage, tongue, and tendon. The results suggest that for the tissues with higher stiffness, cavitation was initiated primarily by the negative pressure of the incident wave, since higher tissue stiffness tends to suppress bubble growth, limiting the ability of incidental bubbles to effectively scatter shocks. Because repeated bubble expansion and collapse causes the tissue fractionation in shock-scattering histotripsy, even if a bubble cloud is generated, stiffer tissues may yet hinder bubble expansion enough to prevent effective fractionation using shock scattering histotripsy. The stiffness of the tissue therefore not only affects the threshold, but the amount of damage done [35]. Other tissue properties found to increase tissue susceptibility to histotripsy damage were higher average water content, lower density, lower ultimate stress, and higher ultimate fractional strain.

As with intrinsic threshold histotripsy, the period between successive HIFU pulses has a significant impact on the rate of tissue erosion in shock scattering histotripsy. Xu *et al.* [3] saw that higher PRFs and longer pulse lengths were less efficient at eroding tissue, and Wang *et al.* [53] showed that the spatial locations of nuclei persisted between pulses at higher PRFs, reducing treatment efficiency due to "cavitation memory". Increasing the time between the pulses resulted in more homogenous regions. In addition to the persistence of nuclei between pulses, the bubble cloud can itself persist for over 50 ms, and these persistent bubbles can shield the focal zone from subsequent shocks, preventing complete fractionation of tissue [60].

An interesting aspect of shock-scattering histotripsy in liquids or areas of fully fractionated tissue is the occurrence of considerable streaming through the focal region in direction of HIFU propagation, caused by acoustic radiation force associated with histotripsy pulses. A pair of studies by Park *et al.* [61] and Maxwell *et al.* [62] employed particle image velocimetry (PIV) to measure the streaming velocity field induced by histotripsy in an *in vitro* phantom mimicking venous blood flow. Histotripsy pulses comprising 5 to 20 cycles were transmitted for a range of pressure amplitudes sufficient to induce cavitation clouds at the focus, which was positioned in the middle of the vessel phantom. The velocities at the focus ranged from 12 to 120 cm/s and increased with pulse duration, PRF and pressure amplitude, as may be expected. Importantly, streaming velocities were greatly enhanced at pressures above the threshold for histotripsy, owing to scattering of the HIFU beam by the bubbles and the resulting acoustic radiation force. A vortex ring formed about the focus to provide return of the streaming flow, as the flow was bounded in the direction of HIFU propagation by the vessel wall.

2.3 Boiling histotripsy

Boiling histotripsy is based on enhanced absorption at the shocks in HIFU waveforms at the focus leading to rapid localized heating and formation of a large primary vapor bubble, as illustrated Figs. 2(g)-(i). Formation of such a millimeter-sized vapor bubble at the focus in under 10 ms was first observed in transparent polyacrylamide gels and was supported by numerical predictions of heating using both the bioheat equation, which accounts for diffusion effects, and weak shock theory, in which the heat deposition is proportional to the cube of the shock amplitude, the tissue's coefficient of nonlinearity, and HIFU frequency, and temperature elevation grows linearly with time [13]. Both methods predicted the time to reach boiling at the focus of less than 10 ms and the results agreed well with each other, confirming that heat diffusion did not play any significant role in case of such rapid heating. It was then hypothesized and later confirmed in soft tissues that if the HIFU burst duration slightly exceeds the time to reach boiling, and is less than 20 ms, with duty cycle less than 1% tissue at the focus is fractionated into subcellular debris without discernable thermal effects [10, 11, 31]. The absence of measurable thermal denaturation may seem somewhat paradoxical, given the expected temperature rise at the focus to 100°C. However, this temperature rise is not only very rapid, but also highly spatially confined to a central region of the focus where shock fronts occur, approximately 100 microns in width [13]. The volume of the ensuing vapor bubble is orders of magnitude larger, and the subsequent mechanisms of tissue fractionation described below are non-thermal. In some respect, this vapor bubble plays a similar role as the initial incidental bubble in shock-scattering histotripsy: it creates a pressure release boundary for the remaining shockwaves, and, consequently, leads to the formation of a layered bubble cloud proximal to the vapor bubble via shock-scattering [11, 14, 63]. The remaining burst is much longer than in shock-scattering histotripsy, which alters the mechanisms of tissue fractionation. Simon et al. [15] showed that when such milliseconds-long bursts of shockwaves were incident onto tissue-air interface (i.e. the vapor bubble surface), tissue debris could flow like fluid to create a miniature acoustic fountain – ejection of micron-sized tissue fragments into the void, also termed acoustic atomization – resulting in a small area of fractionated tissue. It was also demonstrated that the cavitation cloud proximal to the pressure release boundary was a necessary component of the atomization phenomenon, because when static overpressure was applied, no fractionation and only thermal denaturation occurred in bovine liver [64]. Most likely this cavitation activity serves to weaken the tissue at the surface of the vapor bubble and aids ejection of its fragments. Another mechanism shown necessary for successful atomization was tissue surface wetting, most likely through formation of capillary waves within the wetted layer and areas of subsurface cavitation within them [64].

Unlike shock-scattering and intrinsic threshold histotripsy, where areas of fractionation merge together over the course of the treatment to form a contiguous void, boiling histotripsy lesions start as a small fractionated area that is enlarged by subsequent pulses until its size plateaus [31]. The shape of the lesion starts out with a small ovoid shape and then gradually develops into a tadpole shape [65]. The "head" of the tadpole is proximal to the HIFU focus and is hypothesized to be formed by the combined effects of atomization and cavitation. The "tail" is formed by the expansion of the initial vapor bubble, the impact of tissue fragments ejected from the proximal side of the bubble that could reach velocities

of up to 15 m/s [64], and formation of secondary boiling bubbles distal to the focus due to the diffraction of the incoming HIFU waves on the original bubble [14], as shown in Fig. 2(i). Thus, the dependence of boiling histotripsy lesion size and shape on the parameters of the HIFU field is more complex than it is for intrinsic and shock-scattering histotripsy, but the general trends are similar: lesions are larger at lower HIFU frequencies [11] and longer pulses [25], and are shorter and wider for more focused transducers, i.e. lower *F*-numbers [66]. The dimensions of single boiling histotripsy lesions produced by a given transducer are typically larger than in shock-scattering and hybrid histotripsy [25, 65].

As mentioned above, the main requirement to the focal waveform in boiling histotripsy is that the shock amplitude is sufficient for reaching 100°C in under 10 ms; for most tissues this implies the shock amplitude being over 60 MPa, for frequencies higher than 1 MHz. Typically boiling histotripsy exposures utilize the output power at or above formation of fully developed shock – when the focal peak positive pressure p_+ equals shock amplitude [51]. The shock amplitude is defined in this case as a pressure jump within the steepest part of the acoustic waveform, between the time points where the time derivative of pressure decreases to a certain value, typically 2.5% of the maximum value [67]. With this definition, it has been shown that shock-wave heating predicted by the weak shock theory corresponds well to the heating calculated in direct numerical simulations [13, 67]. Conversely p_- is ideally kept low, to avoid the formation of incidental bubble clouds prefocally. Those bubbles may shield the focus and prevent the initiation of boiling, yet produce little to no mechanical disruption by themselves [17]. Due to their incidental nature, the threshold for prefocal bubble formation decreases with HIFU frequency.

2.4 Hybrid histotripsy

Hybrid histotripsy, as the name implies, uses pressure amplitudes between what is commonly found in shock-scattering histotripsy and boiling histotripsy, and pulse lengths of 200-1000 μs to fractionate tissues, while duty cycle usually remains similar at the 0.5-2%. Peak negative pressures are typically on the order of 15-20 MPa; higher peak negative pressures are used in tough, collagenous tissues like tendon. As a result, boiling temperatures are not reached within every pulse, although may be reached at some point during treatment. In hybrid histotripsy, heat is hypothesized to “soften” the target tissue to make it more susceptible to cavitation-induced damage, as well as to promote cavitation bubble growth and facilitate shock scattering. Thus, some degree of thermal denaturation is often intentionally present in the fractionated tissue homogenate, but not necessarily at the lesion borders [23, 24].

In 2018, Eranki *et al.* [23] demonstrated hybrid histotripsy with a 1.2 MHz transducer array, p_+=100 MPa and p_-=18 MPa, and pulse length of 666 μs in *ex vivo* heart, kidney, and liver. Tissue temperature measured during treatment with MR-thermometry reached 50-55°C at the focus, which was in good agreement with calculations for weak shock theory and heat transfer. In 2016 Guan *et al.* [24] used lower amplitude bursts of shock waves (p_+=35 MPa and p_-=8 MPa) at 1.06 MHz in a two-stage regime combining 200-μs and 500-μs pulses delivered at 100 Hz with strategic pauses to first emphasize heating to generate cavitation nuclei and then form a homogenate. The appearance of boiling

bubbles was confirmed in polyacrylamide gels approximately 6.6 seconds into the first stage, significantly increasing inertial cavitation as observed through passive cavitation detection (PCD). When treatments were extended to *ex vivo* porcine kidney and paused at the end of stage one, only partial fractionation with thermal denaturation was observed. However, when the treatment progressed to stage 2, cavitation energy was found to increase and fully liquified tissue homogenate with a smooth boundary was produced. The authors postulated that creating the boiling bubble in stage 1 was essential towards increasing the number of bubble nuclei, which along with the reduction in viscosity as the focal liquefied volume contributed to the success of fractionation at relatively low pressure amplitudes.

Another advantage of hybrid histotripsy vs boiling histotripsy was increased ablation rate demonstrated in *ex vivo* large-volume hematomas [25]. The same 1.5-MHz, transducer with *F*-number of 0.75 was used to deliver 10- or 2-ms pulses for boiling histotripsy (p_+=120 MPa and p_-=17 MPa, time to boiling 1.85 ms) or 400-μs pulses at higher amplitude for hybrid histotripsy (p_+=148 MPa and p_-=21 MPa, time to boiling 0.55 ms) at a 1% duty cycle. Although hybrid histotripsy lesions were smaller, they formed faster and had a more regular ovoid shape facilitating efficient beam scanning and higher liquefaction rate of 2.62 mL/min vs 0.68 mL/min for boiling histotripsy.

Hybrid histotripsy has also been used in very stiff, collagenous tissues resilient to the three other forms of histotripsy. In an investigation of histotripsy of tendons [68], it was shown that 1-ms pulses delivered at 1% duty cycle for 60 seconds (1.5 MHz, p_+=89 MPa and p_-=26 MPa, time to boiling 2 ms) caused mild mechanical microdamage in the form of fiber separation without observable thermal injury. When the amplitude and duty cycle were kept constant, but pulse duration increased to 10-ms, the same effect was observed for 15-second treatment, but not 30-second treatment, where thermal denaturation was observed. There is thus a delicate balance in the dynamics of thermal dose delivery when facilitating histotripsy of such tissues, and hybrid histotripsy parameters appear to be optimal in that regard.

2.5 Emerging histotripsy techniques

A few modifications to the histotripsy techniques described above were recently reported – pressure-modulated shockwave histotripsy (PSH) and steered-focus histotripsy (SFH) [69-72]. PSH is a form of boiling histotripsy that uses 5-34 ms pulses with reduced pressure amplitude after the predicted time-to-boil [70]. The goal of PSH is to create and maintain the boiling bubble without significant shock scattering for better control of the size and shape of the resultant lesion. A recent study in the *in vivo* murine liver showed for the same pulse length and number of pulses, that PSH produced approximately 2.37-fold shorter and 1.35-fold narrower lesions vs boiling histotripsy [71]. The increased control of PSH over traditional, constant amplitude boiling histotripsy, may be useful for miniature targets, as well as locations adjacent to sensitive structures. Conversely, the goal of steered-focus histotripsy is to accelerate ablation through axially extending the bubble cloud, in both boiling and intrinsic threshold histotripsy [69, 72]. The cloud is extended within each pulse by steering the HIFU focus towards the transducer after initiation of boiling or intrinsic threshold bubble cloud and utilizing the shock-scattering effect. The increase of ablation rate is thus dependent on the transducer array design and the axial steering range within which

sufficient shock amplitude is achievable. For example, a 3-fold acceleration of volumetric ablation was reported for steered-focus boiling histotripsy in *ex vivo* tissue [72].

3. METHOD-SPECIFIC INSTRUMENTATION DESIGN CONSIDERATIONS

Several examples of transducers for histotripsy are shown in Fig. 3. Histotripsy sources use piezoelectric materials for generating ultrasound pulses, such as the piezoceramic lead-zirconate-titanate (PZT), or piezocomposites which embed small piezoceramic elements within a polymer matrix. When a high voltage excitation signal is applied to the material, a mechanical deformation results, and ultrasound is radiated from the surface of the element. Methods for focusing these fields at a fixed location include forming the piezoelectric element into the shape of a spherical cap (e.g., as shown in Fig. 3(b), adapted from [73] or Fig. 3(f)) which creates a geometric focus at the center of the radius of curvature, or coupling flat transducer elements to an acoustic lens, which simplifies the fabrication of the piezoelectric element (e.g., as in Figs. 3(c) and 3(d), corresponding to refs. [74] and [50]). Alternatively, electronic focusing and beam steering can be implemented by using an array of elements and controlling the phases of the excitation voltage waveforms for each element, such that constructive interference results in maximum pressure at the desired focal location (Fig. 3(a), adapted from [75] and Fig. 3(e), based on [76]) The use of electronic focusing and steering provides the ability to scan the treatment region throughout the target volume without the need to physically move the transducer, as well as allowing for aberration correction when beams are transmitted through inhomogeneous media. Most systems also incorporate an ultrasound imaging probe coaxially aligned with the HIFU focus for targeting and treatment guidance, as seen in the center of the transducers shown in Figs. 3(b), (e), and (g).

Characteristics of the instrumentation used for each histotripsy method will be different due to the differences in underlying physical mechanisms and differences between targets. First, the desired propagation characteristics influence how strongly focused the transducer is, as represented by its *F*-number. Whereas nonlinear propagation of the excitation pulse is to be avoided in the intrinsic threshold approach, nonlinear propagation is necessary for generating the shocks in boiling histotripsy and shock scattering histotripsy. Accordingly, many studies involving intrinsic histotripsy, where nonlinear propagation is best avoided, use more strongly focused transducers, with *F*-numbers of about 0.6 to 0.75 [21, 44, 45, 77], while shock-scattering histotripsy frequently uses less focused transducers, with *F*-numbers between roughly 0.7 and 1.0 [2, 3, 78-80]. Note that histotripsy transducers are commonly suitable for operation in more than one regime. For instance, the transducers illustrated in Figs. 3(c) and 3(d) have been successfully used for both shock-scattering histotripsy and boiling histotripsy [33, 65, 74, 81, 82]. Boiling histotripsy tends to use larger *F*-numbers, roughly between 0.8 and 1.5 [11, 31, 37, 66, 74, 76], which are beneficial for generating the high amplitude shocks needed for millisecond boiling. An array designed for boiling histotripsy in abdominal targets comprising 256 elements arranged on a spherical cap is shown in Fig. 3(e) and was used for the studies reported in [16] and [76]. The array was designed for operation at 1.5 MHz, with a nominal focal length of 12 cm and *F*-number of 0.83. An example of a smaller single-element transducer for boiling histotripsy is shown in

Fig. 3(f) and was used in the studies reported in [11], [13] and [10], operating at 2 MHz with an aperture of 4.4 cm and *F*-number of 1.0.

While the focal length of the transducer is dictated largely by the depth of the treatment target, the desired *F*-number for an application therefore dictates the aperture used for the transducer. In general, transducer arrays used for intrinsic threshold histotripsy have the largest apertures, which can be in the range of approximately 10 cm to 20 cm [44, 45, 77], although smaller transducers have been used for *in vivo* experiments in rodents [83]. Shock scattering histotripsy tends to use transducers with apertures of about 10 cm to 15 cm [36, 79, 80]. Boiling histotripsy can be realized using the smallest transducer apertures, in the range of approximately 4 cm to 14 cm [11, 25, 33, 37, 76, 84, 85].

The availability of acoustic access can also limit the size of the transducer which can be used. For instance, when creating precise lesions in the brain transcranially using intrinsic threshold histotripsy, strongly focused hemispherical arrays covering a large portion of the skull can be employed and are advantageous because of the high focusing gain. Conversely, in considering ablation in the prostate, where extracorporeal acoustic access is limited, small transducers that could be used transrectally are advantageous. Fig.3(g) shows a single-element 2 MHz transducer with a focal length of 4 cm and an aperture of 5.0 mm × 3.5 mm that was designed for prostate ablation via boiling histotripsy [86-88].

Implementation of electronics for powering histotripsy transducers has multiple challenges, and requirements for acoustic power, transducer electrical input impedance, and number of array elements must all be considered. First, although the time-averaged power is usually on the order of a few watts, the required peak acoustic power levels for histotripsy can range from hundreds of watts to several kilowatts [25, 79]. Attenuation in tissue, especially for deep targets, increases the amount of acoustic power that must be generated by the transducer to maintain the same focal pressure. For arrays, independent driving channels for each transducer element are desirable so that the timing of each element can be varied for electronic focusing and beam steering, making class-A amplifiers prohibitively expensive for arrays with large numbers of elements. Intrinsic histotripsy, requiring the shortest pulses and highest p_- of the four methods, generally has the highest peak power requirements. In a 2006 study [89], Hall and Cain introduced a switching amplifier using MOSFETs in a half-bridge configuration, with 512 independent channels, which was used in early studies for both intrinsic threshold histotripsy and shock scattering histotripsy [9, 21]. The output of the MOSFETs were connected to the transducer elements through a set of tuned output filters, allowing for voltages of over 1 kV to be applied to the transducer elements. The amplifier was designed to deliver 20 W of power to each output channel for pulses less than 100 μs but was also capable of running in continuous-wave mode at lower power levels. Each of the amplifier channels was driven by a microcontroller implemented on a low-cost FPGA.

An advantage of boiling histotripsy is the use of lower peak power levels, with values reported for several *in vivo* studies between 240 W and 650 W [25, 30, 37, 85]. These correspond to time-averaged power values of 2.4 W to 6.5 W, when operating at a duty cycle of 1 %. These lower power levels allow for lower voltages to be used, and, in turn,

more flexibility in the design of the driving electronics. For single-element transducers, commercial off-the-shelf RF power amplifiers can be used for benchtop proof-of-concept experiments [11]. Other studies on boiling histotripsy *in vivo* have successfully used the commercially developed Alpinion VIFU-2000 preclinical system (Alpinion Medical Systems, Bothell, WA, USA) operating at peak power levels between 25 W and 600 W [84, 85]. On the other hand, use of custom electronics also allows for electronic control of the excitation signal timing for each array element, for instance when adjusting element phases to adjust for aberrations when propagating through inhomogeneous layers [33]. At higher power levels, the long pulses used can cause amplifier output voltage to droop over the duration of the pulse. The half-bridge amplifier design described in the previous paragraph was modified for use in boiling histotripsy by Maxwell *et al.* [74], where a pulse length of 10 ms would otherwise cause an unacceptable amount of voltage drop. To address this, an external capacitor bank was used to store the energy required for the long bursts, with a net capacitance of 9 mF chosen so that the voltage across the capacitors would drop by no more than 10% for a 10000-cycle pulse at 1 MHz. A tuned array of smaller bypass capacitors and damping resistors was added in parallel with the energy storage capacitors to prevent a resonance resulting from the energy storage capacitors and their self-inductance.

For MR-guided applications, the use of MR-compatible materials must be used for the transducer to ensure both patient safety and image quality, precluding the use of ferrous metals. The total amount of metal should be minimized in such cases. A system for transcranial MR-guided histotripsy has been recently developed at University of Michigan [44], using sintered PZT elements with 3D printed polymer housings and matching layers, and a nylon frame. Commercially available systems designed for MR-guided HIFU have also been successfully used for boiling histotripsy and hybrid histotripsy, in both *ex vivo* and small animal *in vivo* studies [23, 30, 37, 90]. Clinical systems Sonalleve V1 and V2 (Profound Medical Inc, Mississauga, Canada) use a 256 element array operating at 1.2 MHz capable of acoustic peak power levels of up to 1000 W, with *F*-numbers of 0.94 and 1.03, respectively [91]. A preclinical Image Guided Therapy system (IGT, Pessac, France) uses a 3 MHz annular transducer array with 48 mm diameter and F-number variable within 30-80 mm range, driven with electrical power of up to 350 W [90, 92].

Towards endoscopic histotripsy, miniature high frequency focused actuators with apertures of 1 cm or less have recently been developed by a research team at Dalhousie University [73, 93-96]. An example of one such transducer is illustrated in Fig. 3(b) [73]. The transducer uses a planar PZT-5A piezoelectric element operating at 6.3 MHz, coupled to an aluminum focusing lens designed for focusing at 6 mm coated with a parylene matching layer. A 4 mm by 4 mm square hole in the center of the therapy array contains a co-registered imaging array for image guidance at 30 MHz. The transducer could generate peak negative pressures greater than 28 MPa and was successfully used to ablate *in vivo* rat brain tissue, and histology results revealed complete ablation in regions with submillimeter dimensions.

The maximum acoustic power that can be transmitted by a piezoelectric transducer is constrained by multiple factors. First, piezoelectric materials are subject to voltage limits which should be adhered to for linearity of mechanical displacement with respect to the excitation voltage, commonly on the order of 100 V per millimeter of thickness

[97, 98], while high-voltage piezoelectrics are capable of operating at several kilovolts per mm of thickness. The voltage rating of wiring and other insulating components must also be considered. A more relevant concern with histotripsy transducers is heating due to dissipation in the piezoelectric elements. Many piezoelectric materials lose their crystal structure, along with their piezoelectric properties, above the Curie temperature – a phenomenon known as “depoling”. For pure PZT crystals complete depoling occurs around 350 °C, although electromechanical coupling may be degraded at temperatures well below this upper limit. Additionally, many piezoelectric ceramics are not pure but have specific impurities added to alter their electrical or mechanical properties, which can reduce the maximum operating temperature. Further, many of the other construction materials such as adhesives, matching layers, and polymer lenses will have much lower temperature limitations which need to be considered when operating at high power levels. This may be particularly true for piezocomposite transducers, where small piezoelectric pillars are embedded in a polymer matrix. Maximum operating temperatures of 60 to 70 °C are common. Thus, when designing transducers for histotripsy, limitations of maximum working temperatures, voltages and output power should be carefully considered.

4. CLINICAL APPLICATIONS OF DIFFERENT HISTOTRIPSY METHODS

The noninvasive nature and uniqueness of histotripsy bioeffect have resulted in a large number of clinical applications where its use is currently being investigated in *ex vivo*, preclinical and clinical studies. There is a substantial overlap between histotripsy techniques that can be equally efficiently applied to targets that are mesoscale, i.e. approximately 0.5-3 cm in size, located superficially or have an acoustic window unobstructed by bowel and bone, and are cellular rather than fibrous or calcified. In targets with characteristics outside of the realm specified above some part of the histotripsy spectrum may be preferable. Thus, the applications discussed below in the context of the optimal part of histotripsy spectrum are grouped by those three characteristics – target size, acoustic access, and tissue stiffness and toughness.

Histotripsy applications in acoustically accessible, soft, mesoscale targets.

As mentioned before, in those targets most histotripsy techniques are equally applicable and produce similar outcomes. Examples of those applications include subcostal or partially transcostal ablation of soft tumors in the liver and kidney [33, 99, 100], superficial tumors in veterinary patients [101], tumor ablation in small animal experiments to study the downstream immune effects of histotripsy [34, 85, 102-105], and liquefaction of soft superficial targets other than tissue – hematomas and abscesses [81]. These targets are accessible with transducers that can be large and/or strongly focused, and the size of the focus in all cases can be controlled by the choice of the transducer operating frequency and *F*-number – within feasibility limits of each technique.

Histotripsy applications in intraluminal applications and/or with restricted acoustic window.

Ablation of prostate, both in the context of benign prostate hyperplasia (BPH) therapy and local cancer therapy, is a representative example of an application with challenging

extracorporeal acoustic window, but unobstructed endorectal access. The reduction of prostate volume through histotripsy liquefaction for relieving the symptoms of BPH was the first application of histotripsy to be tested in a Phase I clinical trial [106]. In acute and chronic preclinical studies that preceded that trial shock-scattering histotripsy ablation of healthy canine prostate was successfully performed transabdominally, under endorectal ultrasound imaging guidance, with a 700 kHz transducer (13 cm aperture, *F*-number of 0.85) [107]. However, the pilot trial of a prototype clinical device – Vortx Rx - that built on those results did not produce measurable debulking of prostate volume in 25 BPH patients, although a hyperechoic bubble cloud was observed on ultrasound imaging. A number of factors were hypothesized to contribute to this discrepancy, the most important one being the absence of adequate acoustic window (i.e. path unobstructed by bones) to the human prostate transperineally.

Transrectal approach, which has been used in thermal HIFU clinically for many years, is much more preferable with regards to unobstructed acoustic window, but requires miniature transducers that typically operate at higher (3-4 MHz) frequencies to increase focal gain and heat deposition [108]. The surface area of those transducers, to date, has been deemed insufficient to achieve focal pressures required for shock-scattering histotripsy at lower frequencies that would provide clinically relevant ablation rate. However, focal pressure levels required for boiling histotripsy are lower, and were recently shown to be achievable with a 2 MHz transrectal transducer (Fig. 3) similar in size and shape to clinical HIFU devices [86, 88]. The shock front of 80 MPa amplitude was achieved at 130 W peak acoustic power, which was less than 30% of the maximum power allowed for by the manufacturer. Successful boiling histotripsy ablation of canine prostate *in vivo* using this transducer, under coaxial ultrasound imaging guidance, was also recently demonstrated [109]. The success of this approach warrants further investigation of achievable pressures with transducers of even smaller size and/or lower frequency for endoluminal or interstitial applications such as transvaginal ablation of uterine fibroids [110], endoscopic ablation of targets in the heart, liver and pancreas [111, 112] and catheter-based ablation in the brain [113] that have been investigated in thermal HIFU, but not histotripsy.

An important consideration in applications with restricted acoustic window is deviation of the transducer geometry from the spherical bowl shape typical in thermal HIFU to conform to the available acoustic window and sonication geometry. One option is to truncate the spherically symmetric transducer in elevational dimension of the in-line ultrasound imaging probe. This truncation facilitates subcostal, i.e. highly angled access to targets in the liver and kidney, and better co-localization of the US imaging plane with the 3D HIFU field. This subcostal approach is important around gas-filled organs (e.g. bowel gas, lungs) that are easily damaged by the therapy field, yet may not be visible on the in-line 2D US imaging [101].

Fibrous tissues with high stiffness and toughness

Tissue stiffness is expressed via its elastic modulus, defined as the ratio of shear stress to resulting strain; tissue toughness characterizes the stress necessary to cause a fracture, in other words – how brittle the tissue is. High tissue stiffness has been shown to reduce

the efficiency of histotripsy treatments in a number of works [35, 43, 49, 101], potentially due to the suppression of bubble growth, whereas the importance of toughness has been somewhat overlooked until recently [114]. Connective tissue with high concentration of collagen and/or elastin fibers is both stiff and tough and is present in many pathologic tissues such as BPH and prostate cancer, uterine fibroids, pancreatic tumors and metastases thereof, cholangiocarcinoma, scar tissue, as well as healthy tissues such as tendons, ligaments, cartilage and fascia. All of the above tissues are targets for histotripsy, but the outcome goals may be different: complete fractionation in the case of tumors vs induction of sparse and localized areas of damage to promote healing response (tendons, ligaments and cartilage), softening (scars and strictures) or puncturing of cyst walls.

BPH tissue is perhaps the most thoroughly studied fibrotic tissue in terms of its resistance to histotripsy damage. In the clinical trial of shock-scattering histotripsy in patients with BPH mentioned above [106] one of the hypothesized reasons for the absence of fractionation effect was the fibrous nature of BPH. In a recently published mechanistic study of bubble dynamics during shock-scattering histotripsy at 700 kHz in hydrogels with high toughness the effect of “cavitation memory” – non-dissolution of bubbles between pulses and their occurrence in the same place at every pulse -was found to impede full fractionation at higher PRFs, but not in the agarose gel with equivalent stiffness [114]. The same high-PRF exposures in resected human BPH samples similarly resulted in areas of isolated damage rather than contiguous fractionated lesions. One potential explanation of this effect of high tissue toughness is that the collapsing bubbles cannot break the highly pliable fibers to migrate and merge together to form larger bubbles that could potentially be more efficient. Conversely, boiling histotripsy exposures of autopsy human prostate tissue with BPH at 1.5 MHz achieved full fractionation of the targeted area [115]. It was also confirmed that human prostate (both healthy and with BPH changes) required more pulses per focus for full fractionation compared to canine prostate reported by Sekar et al. (60 vs 15 pulses, treatment time 60 vs 15 seconds), likely due to its much more fibrous nature [109] . Several factors could contribute to the higher efficiency of boiling histotripsy in this application, including more dramatic damage occurring within a single pulse due to atomization and streaming, lower PRF that provides the time for bubbles to dissolve, and the localized heating component that could cause partial collagen hydrolysis reducing its toughness. The latter mechanism was reported by Smallcomb et al. [32] when hybrid histotripsy approach was found to be somewhat successful in disrupting tendons through a combination of heat causing partial or complete collagen or fibrin hydrolysis, and cavitation, which can successfully fractionate the partially-hydrolyzed fibers. Taken together, these studies suggest that boiling histotripsy and hybrid histotripsy are more efficient than shock-scattering histotripsy in breaking tough collagenous tissue.

In comparing shock-scattering and intrinsic threshold histotripsy in fibrous tissues, per recently reported study in resected human uterine leiomyomas, shock-scattering histotripsy with 5-cycle pulse duration only achieved the formation of scattered areas of disruption within targeted tissue, similarly to BPH [116]. Intrinsic threshold histotripsy exposures resulted in more defined (i.e. less diffuse) bubble cloud, as per US imaging, and achieved full fractionation, albeit only at a very large treatment time, over 100 times over that required for soft tissue ablation. It should be noted, however, that the 5-cycle pulses were

delivered at higher PRF compared to single-cycle pulses, which may have confounded the comparison. Another interesting aspect of this study was the presence of coagulative necrosis, along with liquefactive necrosis in all successful exposures, further supporting the concept of using heat to enhance fractionation.

Another stiff and tough material relevant to histotripsy is retracted intravascular clot in the context of deep vein thrombosis (DVT) – formation of chronic clots, most often in the legs. The clot composition and mechanical properties change over time, from fairly soft and brittle fresh clots consisting of highly porous fibrin matrix with a large number of embedded red blood cells (RBCs) and high water content to stiffer and tougher retracted clot with more compacted fibrin structure, fewer pores and lower water content. Fresh clots are relatively easy to fractionate with both shock-scattering or intrinsic threshold histotripsy [20, 57]; however, fractionation becomes much more challenging in aged and retracted clots, and requires more histotripsy pulses to be delivered [117]. Combination of histotripsy with common clot lytic of recombinant tissue plasminogen activator (rt-PA) was shown to accelerate treatment [118], as did the increase in p^- up to 35 MPa, i.e. beyond the intrinsic threshold, and the number of cycles within the pulse from 1 to 20 [119]. These results suggest that shock-scattering may be more efficient than intrinsic threshold histotripsy at fractionation of aged clots.

Applications in the brain

The main challenge in using HIFU for thermal ablation in the brain had been high attenuation, reflection and beam aberration by the skull. To address those issues, large, hemispherical transducer arrays operating at low frequency (250-660 kHz) had to be used, algorithms based on CT scans of the skull that allowed for beam aberration correction had to be developed, and even then only 10% of acoustic power would be transmitted towards the focus [120]. Further, ultrasound imaging of those treatments would be impossible for the same reason, which necessitated the use of MR imaging and thermometry for guidance. Nonetheless, ablation at specific locations in the brain to treat essential tremor was among the first clinical indications of HIFU thermal ablation has been successfully performed clinically for the past 10 years. Importantly, however, the transcranial ablation is limited to the targets that are relatively small and located centrally in the brain due to the danger of skull overheating and limitations of electronic beam steering. The latter limitation is dictated by the increase of the relative amplitude of side lobes and the necessity to compensate for focal intensity decrease with electronic beam steering away from the geometric focus. Various efforts to enlarge the treatment envelope have been undertaken, but the ultimate solution has not yet been found.

Based on the geometry of the problem, the most suitable histotripsy type for transcranial ablation is intrinsic threshold histotripsy, as it uses large, hemispherical, low frequency transducers, similarly to transcranial thermal HIFU. Clinical applications include ablation of brain tumors and liquefaction of subdural and intracranial hematomas for subsequent drainage. The feasibility of transcranial intrinsic threshold histotripsy of healthy brain and liquefaction of hematomas has been demonstrated *ex vivo* and *in vivo* in a porcine model with craniectomy, through human skull [19, 121, 122]. Two systems were developed, the

earlier one using a 500 kHz, 256-element hemispherical array, and subsequently - an MR-compatible 700 kHz 128-element array with *F*-number of 0.75, both with 15 cm focal distance. It was demonstrated that fractionated lesions up to 1 cm in size could be safely produced in pig brain without overheating the skull, per MR thermometry, as close as 5 mm away from the skull surface. This ability to enlarge the electronic focus steering range (and thus increase treatment envelope) is due to the fact that side lobes are not a concern for the very short, half-cycle pulses used in intrinsic threshold histotripsy, and also because there is more headroom to compensate for intensity decrease, as time-averaged acoustic power remains low. Beam aberration by the skull is equally relevant in transcranial histotripsy as it is in thermal HIFU, and necessitated the development of a phase correction approach [123-125]. The approach will be described in more detail below (in the section on current challenges) but is based on producing a cavitation bubble by a single histotripsy pulse, and passively listening to its collapse with all the elements of the transducer array.

The inability to utilize ultrasound imaging for real time treatment guidance in transcranial histotripsy treatments has led to the development of alternative ways to target the treatment, monitor its progression and evaluate completeness, based on MRI and stereotactic navigation. Although those methods are not as mature as ultrasound imaging-based guidance, this is currently an area of active research [126].

Although the feasibility of other histotripsy regimes has not yet been experimentally investigated for transcranial brain ablation, a recent numerical simulation study suggests that the formation of shocks of over 60 MPa amplitude is achievable using a 1 MHz transducer with a radius of curvature of 20 cm and *F*-number of 1 without exceeding the technical limitation of 40 W/cm^2 at the transducer surface [127]. If proven experimentally, the use of those less focused transducer arrays could simplify access to different areas of the brain and acoustic coupling vs hemispherical arrays due to the increased ability to mechanically shift and rotate the transducer around the skull.

Applications in miniature targets

Transcranial histotripsy in preclinical rodent models of brain cancer is one of the applications in which the size of an individual histotripsy lesion has to be very small, in the submillimeter to a millimeter range, whereas the ablation rate is not as big a concern [73]. Importantly, in those situations the lesion sphericity, i.e. its axial dimension being similar to lateral, is an advantage. This is also relevant in other preclinical studies in rodents such as investigation of immune response following ablation of small orthotopic tumors in kidney and liver [83, 85], subcutaneous tumors [4, 101, 103], histotripsy-based liver decellularization for intrahepatic cell delivery [34], and release of tumor-specific intracellular biomarkers into the circulation [84]. The use of all histotripsy types was demonstrated to be feasible in those scenarios, while necessitating the use of the upper bound of frequencies specific to each histotripsy type, e.g. 6 MHz for intrinsic threshold histotripsy [73], 1 MHz for shock-scattering histotripsy, and 1.5-3.5 MHz for boiling histotripsy, and lower bound of *F*-numbers, i.e. more focused transducers. While lesion miniaturization, especially in the axial dimension, was shown to be feasible for boiling and hybrid histotripsy through shortening of pulses and/or reduction of the number of pulses

delivered per location, shock-scattering and intrinsic threshold histotripsy allow to achieve higher degree of miniaturization [73, 83].

Another histotripsy application requiring miniaturization of lesions is thrombolysis, in particular in the context of DVT, where blood clots can span tens of centimeters in length, but are only 4-6 mm in diameter. In those treatments it is imperative that the endothelial lining of the blood vessel not be damaged, and full liquefaction of the clot is not required, as long as some degree of recanalization is achieved. Thus, the entirety of the bubble cloud should preferably be confined to the interior of the clot. This confinement is most easily achieved with shock-scattering and intrinsic threshold histotripsy types, and both were investigated in this context [20, 57, 117, 128], with the latter showing superior safety profile relative to the former in some of the studies. On the other hand, as mentioned previously, old DVT clots become very tough and shock-scattering histotripsy appears to be more efficient at breaking them [119]; this discovery warrants further investigation into the optimal regime of histotripsy in DVT.

Drilling, puncturing and mixing: histotripsy in liquids and at the surfaces

In most applications described above bulk mechanical ablation of tissues is the ultimate goal of histotripsy exposures; there are other applications that require creating perforations or punctures through membranes, e.g. cyst walls [82] or layers of tissue bordering with fluid, e.g. heart septum ([3, 129]). All these cases imply breaking through tough, elastic tissue layers, in direction perpendicular to the membrane fibers, which corresponds to the HIFU beam axis, from the side bordering with fluid–cyst interior or blood-filled heart chamber. Because part of the bubble cloud is positioned in the fluid, shock-scattering histotripsy has been shown be the most efficient treatment in those applications, i.e. fast formation of puncture with smooth walls through cavitation-based fractionation combined with streaming. When shock-scattering histotripsy at 1 MHz was used to puncture *ex vivo* mimic of ureterocele wall, 0.5-1 mm thick longer pulses (5 vs 2 cycles) created larger punctures (1.2 vs 0.8 mm) within approximately two minutes, likely due to the larger size of the bubble cloud. Conversely, 5 ms long pulses typical for BH did not produce punctures on their own, but enlarged the smaller punctures created by shock-scattering histotripsy to 2.8 mm. High velocity streaming in axial direction inherent to such long pulses was most likely responsible for this effect.

Ultrasound-driven cavitation was known for a long time to result in bacterial kill, both in suspension and in biofilm [130]. It was therefore only natural to apply histotripsy, representing some of the most destructive forms of cavitation, to this problem [81, 131-133]. It is important to note here that bacteria are much smaller than cells (sub-micron vs few microns) and the size of bubbles within the cavitation cloud, which makes them less susceptible to histotripsy damage. Thus, histotripsy cannot be expected to clear infection from the bulk of tissue while sparing the tissue itself; tissue will inevitably be destroyed first. This tissue destruction limits the application of histotripsy to removing biofilms from the surfaces of sturdy implanted materials, such as surgical meshes and catheters, and disinfecting abscesses – walled-off collections of pus and bacteria.

Biofilm forms a protective matrix for bacteria to dwell in that can be tens of microns thick and is very resistant to antibiotic treatment. *Staphylococcus aureus* biofilms grown on the surgical mesh samples used for hernia repairs were shown to be successfully eliminated with an average of 5.4-log kill with shock-scattering histotripsy, whereas the treatment had no effect on the mesh strength [131]. Similar results were reported for clearing bacterial biofilm from the inner surface of ureteral catheters [132] using intrinsic threshold histotripsy. Part of the disinfection effect in those studies could be dislodging or washing bacteria off the biofilm and into neighboring fluid, where they are more susceptible to killing by antibiotics. Both shock-scattering and boiling histotripsy were shown to kill bacteria in suspension *in vitro* and *in vivo* in porcine abscesses, but the kill rate was lower than that reported for biofilms (up to 3-log), likely due to the differences in outcome evaluation (dislodging vs. kill). Furthermore, due to large streaming velocities, longer boiling histotripsy pulses liquefied viscous pus faster than did shock-scattering pulses produced by the same transducer, and a combination of both regimes (liquefy first, disinfect next) was observed to be more beneficial.

5. COMMON CHALLENGES AND FUTURE DIRECTIONS

HIFU beam aberration by soft tissues and bones.

Phase aberrations, i.e., relative phase shifts varying across the HIFU wavefront, arise from the variation in thickness of tissue layers with different sound speed within the acoustic path. Those aberrations result in spatial shift and broadening of the focal area and the decrease of peak focal pressures. Among the soft tissues, fat layers introduce the most severe aberration effects due to the low sound speed – 1420 m/s vs. 1540 m/s for most water-based tissues – and has been long recognized as an important challenge affecting safety, precision and feasibility of thermal HIFU treatments, especially in the kidney and breast [134, 135]. As mentioned earlier, the other major source of aberrations is skull in transcranial applications, as it has varying thickness and high speed of sound compared to soft tissues [120]. Being a HIFU-based technique, histotripsy is also susceptible to the detrimental effects of aberration, although different histotripsy types are affected in somewhat different ways. In general, using lower frequencies and transducers with smaller footprint (i.e. higher *F*-number and/or smaller aperture size) reduces the effects of aberration; techniques relying on shock formation – shock-scattering and boiling histotripsy – are more affected compared to intrinsic threshold histotripsy, as the wavefront has to be synchronized for high amplitude shock formation at the focus [33, 136-139]. Aberrations can be compensated for by using multi-element HIFU arrays and imposing appropriate phase delays on all array elements; the main problem is determining those delays. In transcranial HIFU applications, where brain tissue does not move relatively to the skull, the necessary phase corrections can be determined numerically based on pre-treatment CT scan. However, in soft tissues that move and deform based on patient positioning the corrections need to be determined in real time, immediately prior to treatment. One approach first proposed by Pernot et al. [140] consists of nucleating a cavitation bubble at the focus through a high-amplitude HIFU pulse, and then receiving the acoustic emissions associated with the bubble collapse on all the elements of the HIFU transducer array. The differences in arrival times of those signals to the different elements of the array determine the phase delays necessary to compensate for

aberrations. This approach has been adopted for intrinsic threshold histotripsy treatments, in both transcranial and soft tissue settings and termed acoustic cavitation emission (ACE) [124, 125]. The approach has been successful at recovering a large part of the focal pressure amplitude lost to aberration; the main limitations were related to the destructive nature of the approach and the uncertainty in the spatial position of the nucleated bubble: it could appear anywhere within the focal region, which itself could be shifted due to aberration by up to a few millimeters relatively to the intended target. Recently this limitation was alleviated by using a two-step approach for transcranial treatments, combining CT-based correction with ACE [123].

In an alternative aberration correction approach introduced by Thomas et al. [136] the HIFU array was used in a harmonic imaging pulse/echo mode to receive nonlinear pulses backscattered from the focus. The signals on nearest neighbor elements were cross-correlated to find the relative phase delays, those delays were implemented, and the pulse-echo measurement repeated. Those steps were performed iteratively until the amplitude of the beamsum at the focus was maximized. Depending on the aberration severity 3-10 iterations were required to achieve correction that recovered the majority of focal pressure amplitude within a few seconds. For this approach to be feasible in the presence of physiological motion, synchronization algorithm had to be devised, so that the same scatterers at the focus would be encountered at each iteration [137]. In a free-breathing pig this approach allowed to dramatically reduce the output power required to perform boiling histotripsy ablation in the liver.

Real-time feedback on histotripsy ablation completeness.

Coaxial B-mode ultrasound imaging provides an excellent means of histotripsy ablation planning, targeting and real-time feedback on treatment progression; however, the information on treatment completeness is only qualitative. Because, as mentioned earlier, tissues have inherently variable susceptibilities to histotripsy damage, devising a quantitative, real-time indicator of the degree of tissue fractionation, is of utmost importance. Several approaches to this problem have been proposed to date, primarily based on passive cavitation detection/imaging [13, 43, 118, 141], shear wave elastography (SWE) [81, 142], and color Doppler ultrasound [16, 143]. While metrics derived from passive cavitation detection during histotripsy were shown to correlate with treatment outcome in a number of works [13, 43, 118, 141], they quantify bubble activity rather than the degree of tissue liquefaction resulting from it.

Because histotripsy fractionation results in increasingly softer tissue, it was natural to explore SWE imaging as a quantitative treatment monitoring tool [81, 142]. It was found to be sensitive to treatment progression at the early stages of liquefaction, while the tissue still maintains some elasticity and supports the propagation of shear waves, but not later stages, when it is nearly liquid. In addition, for reliable measurement of shear wave velocity the imaging probe had to be located close to the region being liquefied, thus precluding the use of SWE in the typical coaxial geometry and limiting it to inter-treatment and post-treatment scenarios.

An alternative way to evaluate changes in tissue elasticity is to measure its response to the impact imparted on it by each histotripsy pulse through acoustic radiation force and/or bubble cloud collapse. Intact or partially intact tissue that still maintains its elasticity will rebound, whereas liquefied tissue will not, and may flow in the opposite direction. Thus, ultrafast Doppler imaging realized by the co-axial imaging probe was proposed to measure target tissue motion in response to intrinsic threshold [143] and boiling histotripsy pulses [16]. Because of the differences in pulse duration, the reported tissue motion was also different. Acoustic radiation force induced by milliseconds-long boiling histotripsy pulse causes tissue displacement or liquid streaming away from a transducer during the pulse. Conversely, short intrinsic threshold histotripsy pulses do not impart significant radiation force, but the net motion of asymmetrically collapsing bubbles within the cloud is hypothesized to cause the displacement away from the transducer. After the pulse transfers the momentum to the tissue in both histotripsy methods, the tissue rebounds toward the transducer, albeit at very different velocities - on the order of 1 cm/s for intrinsic threshold and 30–100 cm/s for boiling histotripsy. Therefore, different liquefaction indicators were proposed for the two techniques. For intrinsic threshold histotripsy, the time-to-peak rebound velocity was found to grow and then saturate with tissue liquefaction due to progressively longer lasting bubbles. For boiling histotripsy, the absolute value of the rebound velocity was found to increase from approximately 20 to over 100 cm/s and then saturate as tissue liquefied. Further, the tissue velocity was found to also be dependent on the size of the liquefied lesion: in larger lesions the tissue was observed to flow away from the transducer at velocities exceeding 100 cm/s when fully liquefied. These promising findings warrant further investigation of tissue motion in response to histotripsy pulses and development and validation of quantitative treatment feedback metrics based on ultrafast Doppler.

Alternative imaging guidance methods.

While one of the biggest advantages of all histotripsy approaches is that it can be guided and monitored with ultrasound due to the high change in impedance between soft tissues and bubbles, ultrasound imaging guidance is very difficult when bone is in the ultrasound imaging path. Two big areas where histotripsy is being investigated includes targets behind the ribs and in the brain. Some researchers have turned to magnetic resonance (MR) imaging as an alternative. Anthony et al. [144] compared B-mode ultrasound to T2-, T1- and diffusion-weighted MR imaging after creation of shock-scattering histotripsy lesions in tissues and tissue-mimicking phantoms and found that passive cavitation imaging provided better prediction of liquefaction than post-treatment assessment via B-mode or MR images. They also found that T2-weighted images more accurately reflected liquefaction than post-hoc B-mode imaging. As MR is expected to be particularly useful for brain monitoring, Lu et al. [122] evaluated pre- and post-MR imaging in *in vivo* porcine brain before and after treatment through an *ex vivo* human skull. They found MR-evident lesions were confined within the intended target volume and good correlation between histologically-evident and MR-visible ablation zones. Thus, while MR is potentially feasible to monitor the lesion post-histotripsy therapy, it cannot provide real-time feedback as to the development of the lesion. Additionally, the size and cost diminish some of the point-of-care benefits of an ultrasound-guided histotripsy therapy. Research into cone beam computed tomography

(CBCT) to monitor histotripsy treatment is in its early stages. Towards that end, Kutlu et al. [145] has developed a red-blood cell phantom layered with barium for lesion visualization on B-mode ultrasound and CBCT. Wagner et al. [146] used a combination of CBCT and 2D fluoroscopy to improve targeting and allow for full automation of the histotripsy treatment without ultrasound guidance. CBCT is a promising technology for automating histotripsy treatments; however, it still suffers from lack of real-time feedback as to the progression of the treatment.

6. CONCLUSIONS

Just like most successful tissue ablation methods, histotripsy has evolved into a collection of complementary techniques, each with specific instrumentation requirements, inherent advantages and limitations that only partially overlap. This, in turn, has expanded the number of current and potential clinical applications of histotripsy and facilitated the acceleration of research addressing common challenges of the histotripsy techniques. Given the promising results of the first clinical trials and continued progress in preclinical and instrumentation research, this growth is expected to continue.

ACKNOWLEDGEMENTS

The authors would like to acknowledge the research teams at the University of Washington, Pennsylvania State University and Moscow State University, as well as collaborators from other institutions who have contributed to the development and refinement of histotripsy.

FUNDING

This work was supported by the US National Institutes of Health (R01EB031788, R01AR080120, R01CA258581, R01EB032860, and T32DK007742), and Focused Ultrasound Foundation.

References

[1]. Parsons JE, Cain CA, Abrams GD, Fowlkes JB. Pulsed cavitational ultrasound therapy for controlled tissue homogenization. Ultrasound Med Biol. 2006;32(1):115–29. [PubMed: 16364803]

[2]. Roberts W,W, Hall T,L, Ives K, Wolf JS, Fowlkes JB, Cain C,A Pulsed cavitational ultrasound: A noninvasive technology for controlled tissue ablation (histotripsy) in the rabbit kidney. J Urol. 2006;175(2):734–8. [PubMed: 16407041]

[3]. Xu Z, Ludomirsky A, Eun LY, Hall TL, Tran BC, Fowlkes JB, et al. Controlled ultrasound tissue erosion. IEEE Trans Ultrason, Ferroelect, Freq Control. 2004;51(6):726–36.

[4]. Khokhlova VA, Fowlkes JB, Roberts WW, Schade GR, Xu Z, Khokhlova TD, et al. Histotripsy methods in mechanical disintegration of tissue: Towards clinical applications. Int J Hyperthermia. 2015;31(2):145–62. [PubMed: 25707817]

[5]. Xu Z, Hall TL, Vlaisavljevich E, Lee FT. Histotripsy: The first noninvasive, non-ionizing, non-thermal ablation technique based on ultrasound. Int J Hyperthermia. 2021;38(1):561–75. [PubMed: 33827375]

[6]. Glickstein B, Levron M, Shitrit S, Aronovich R, Feng Y, Ilovitsh T. Nanodroplet-mediated low-energy mechanical ultrasound surgery. Ultrasound Med Biol. 2022;48(7):1229–39. [PubMed: 35351316]

[7]. Khirallah J, Schmieley R, Demirel E, Rehman TU, Howell J, Durmaz YY, et al. Nanoparticle-mediated histotripsy (nmh) using perfluorohexane ‘nanocones’. Phys Med Biol. 2019;64(12):125018. [PubMed: 31071701]

[8]. Loskutova K, Grishenkov D, Ghorbani M. Review on acoustic droplet vaporization in ultrasound diagnostics and therapeutics. BioMed Research International. 2019;2019:9480193. [PubMed: 31392217]

[9]. Maxwell AD, Wang T-Y, Cain CA, Fowlkes JB, Sapozhnikov OA, Bailey MR, et al. Cavitation clouds created by shock scattering from bubbles during histotripsy. J Acoust Soc Am. 2011;130(4):1888–98. [PubMed: 21973343]

[10]. Canney MS, Khokhlova TD, Khokhlova VA, Bailey MR, Ha Hwang J, Crum LA, editors. Tissue erosion using shock wave heating and millisecond boiling in HIFU fields. Proceedings of the 9th International Symposium on Therapeutic Ultrasound; 2009; Aix-en-Provence, France, September 23-26,: American Institute of Physics.

[11]. Khokhlova TD, Canney MS, Khokhlova VA, Sapozhnikov OA, Crum LA, Bailey MR. Controlled tissue emulsification produced by high intensity focused ultrasound shock waves and millisecond boiling. J Acoust Soc Am. 2011;130(5):3498–510. [PubMed: 22088025]

[12]. Khokhlova TD, Wang Y-N, Simon JC, Cunitz BW, Starr F, Paun M, et al. Ultrasound-guided tissue fractionation by high intensity focused ultrasound in an in vivo porcine liver model. Proc Natl Acad Sci USA. 2014;111(22):8161–6. [PubMed: 24843132]

[13]. Canney MS, Khokhlova VA, Bessonova OV, Bailey MR, Crum LA. Shock-induced heating and millisecond boiling in gels and tissue due to high intensity focused ultrasound. Ultrasound Med Biol. 2010;36(2):250–67. [PubMed: 20018433]

[14]. Pahk KJ, Gélat P, Sinden D, Dhar DK, Saffari N. Numerical and experimental study of mechanisms involved in boiling histotripsy. Ultrasound Med Biol. 2017;43(12):2848–61. [PubMed: 28965719]

[15]. Simon JC, Sapozhnikov OA, Khokhlova VA, Wang Y-N, Crum LA, Bailey MR. Ultrasonic atomization of tissue and its role in tissue fractionation by high intensity focused ultrasound. Phys Med Biol. 2012;57(23):8061. [PubMed: 23159812]

[16]. Song M, Thomas GPL, Khokhlova VA, Sapozhnikov OA, Bailey MR, Maxwell AD, et al. Quantitative assessment of boiling histotripsy progression based on color doppler measurements. IEEE Trans Ultrason, Ferroelect, Freq Control. 2022;69(12):3255–69.

[17]. Khokhlova TD, Haider YA, Maxwell AD, Kreider W, Bailey MR, Khokhlova VA. Dependence of boiling histotripsy treatment efficiency on HIFU frequency and focal pressure levels. Ultrasound Med Biol. 2017;43(9):1975–85. [PubMed: 28641910]

[18]. Lin KW, Kim Y, Maxwell AD, Wang TY, Hall TL, Xu Z, et al. Histotripsy beyond the intrinsic cavitation threshold using very short ultrasound pulses: Microtripsy. IEEE Trans Ultrason, Ferroelect, Freq Control. 2014;61(2):251–65.

[19]. Gerhardson T, Sukovich JR, Pandey AS, Hall TL, Cain CA, Xu Z. Effect of frequency and focal spacing on transcranial histotripsy clot liquefaction, using electronic focal steering. Ultrasound Med Biol. 2017;43(10):2302–17. [PubMed: 28716432]

[20]. Zhang X, Owens GE, Gurm HS, Ding Y, Cain CA, Xu Z. Noninvasive thrombolysis using histotripsy beyond the intrinsic threshold (microtripsy). IEEE Trans Ultrason, Ferroelect, Freq Control. 2015;62(7):1342–55.

[21]. Maxwell AD, Cain CA, Hall TL, Fowlkes JB, Xu Z. Probability of cavitation for single ultrasound pulses applied to tissues and tissue-mimicking materials. Ultrasound Med Biol. 2013;39(3):449–65. [PubMed: 23380152]

[22]. Church CC. Spontaneous homogeneous nucleation, inertial cavitation and the safety of diagnostic ultrasound. Ultrasound Med Biol. 2002;28(10):1349–64. [PubMed: 12467862]

[23]. Eranki A, Farr N, Partanen A, Sharma KV, Rossi CT, Rosenberg AZ, et al. Mechanical fractionation of tissues using microsecond-long HIFU pulses on a clinical MR-HIFU system. Int J Hyperthermia. 2018;34(8):1213–24. [PubMed: 29429375]

[24]. Guan Y, Lu M, Li Y, Liu F, Gao Y, Dong T, et al. Histotripsy produced by hundred-microsecond-long focused ultrasonic pulses: A preliminary study. Ultrasound Med Biol. 2016;42(9):2232–44. [PubMed: 27318864]

[25]. Ponomarchuk EM, Rosnitskiy PB, Khokhlova TD, Buravkov SV, Tsysar SA, Karzova MM, et al. Ultrastructural analysis of volumetric histotripsy bio-effects in large human hematomas. Ultrasound Med Biol. 2021;47(9):2608–21. [PubMed: 34116880]

[26]. Prat F, Chapelon JY, Fadil FAe, Sibille A, Theillière Y, Ponchon T, et al. Focused liver ablation by cavitation in the rabbit: A potential new method of extracorporeal treatment. Gut. 1994;35(3):395. [PubMed: 8150355]

[27]. Hu Z, Yang XY, Liu Y, Sankin GN, Pua EC, Morse MA, et al. Investigation of HIFU-induced anti-tumor immunity in a murine tumor model. J Transl Med. 2007;5(1):34. [PubMed: 17625013]

[28]. Kieran K, Hall Timothy L, Parsons Jessica E, Wolf JS, Fowlkes JB, Cain Charles A, et al. Refining histotripsy: Defining the parameter space for the creation of nonthermal lesions with high intensity, pulsed focused ultrasound of the in vitro kidney. J Urol. 2007;178(2):672–6. [PubMed: 17574617]

[29]. Longo KC, Knott EA, Watson RF, Swietlik JF, Vlaisavljevich E, Smolock AR, et al. Robotically assisted sonic therapy (rast) for noninvasive hepatic ablation in a porcine model: Mitigation of body wall damage with a modified pulse sequence. CardioVasc Interv Radiol. 2019;42(7):1016–23.

[30]. Eranki A, Farr N, Partanen A, Sharma KV, Chen H, Rossi CT, et al. Boiling histotripsy lesion characterization on a clinical magnetic resonance imaging-guided high intensity focused ultrasound system. PLOS ONE. 2017;12(3):e0173867. [PubMed: 28301597]

[31]. Wang Y-N, Khokhlova T, Bailey M, Hwang JH, Khokhlova V. Histological and biochemical analysis of mechanical and thermal bioeffects in boiling histotripsy lesions induced by high intensity focused ultrasound. Ultrasound Med Biol. 2013;39(3):424–38. [PubMed: 23312958]

[32]. Smallcomb M, Simon JC. High intensity focused ultrasound atomization and erosion in healthy and tendinopathic tendons. Phys Med Biol. 2023;68(2):025005.

[33]. Khokhlova TD, Schade GR, Wang Y-N, Buravkov SV, Chernikov VP, Simon JC, et al. Pilot in vivo studies on transcutaneous boiling histotripsy in porcine liver and kidney. Sci Rep. 2019;9(1):20176. [PubMed: 31882870]

[34]. Pahk KJ, Mohammad GH, Malago M, Saffari N, Dhar DK. A novel approach to ultrasound-mediated tissue decellularization and intra-hepatic cell delivery in rats. Ultrasound Med Biol. 2016;42(8):1958–67. [PubMed: 27184248]

[35]. Vlaisavljevich E, Kim Y, Owens G, Roberts W, Cain C, Xu Z. Effects of tissue mechanical properties on susceptibility to histotripsy-induced tissue damage. Phys Med Biol. 2014;59(2):253. [PubMed: 24351722]

[36]. Vlaisavljevich E, Owens G, Lundt J, Teofilovic D, Ives K, Duryea A, et al. Non-invasive liver ablation using histotripsy: Preclinical safety study in an in vivo porcine model. Ultrasound Med Biol. 2017;43(6):1237–51. [PubMed: 28318889]

[37]. Wang Y-N, Khokhlova TD, Buravkov S, Chernikov V, Kreider W, Partanen A, et al. Mechanical decellularization of tissue volumes using boiling histotripsy. Phys Med Biol. 2018;63(23):235023. [PubMed: 30511651]

[38]. Fisher JC. The fracture of liquids. J Appl Phys. 1948;19(11):1062–7.

[39]. Temperley HNV. The behaviour of water under hydrostatic tension: III. Proc Phys Soc. 1947;59(2):199.

[40]. Bader KB, Vlaisavljevich E, Maxwell AD. For whom the bubble grows: Physical principles of bubble nucleation and dynamics in histotripsy ultrasound therapy. Ultrasound Med Biol. 2019;45(5):1056–80. [PubMed: 30922619]

[41]. Herbert E, Balibar S, Caupin F. Cavitation pressure in water. Phys Rev E. 2006;74(4):041603.

[42]. Sankin GN, Teslenko VS. Two-threshold cavitation regime. Doklady Physics. 2003;48(12):665–8.

[43]. Vlaisavljevich E, Lin K-W, Maxwell A, Warnez MT, Mancia L, Singh R, et al. Effects of ultrasound frequency and tissue stiffness on the histotripsy intrinsic threshold for cavitation. Ultrasound Med Biol. 2015;41(6):1651–67. [PubMed: 25766571]

[44]. Lu N, Hall TL, Choi D, Gupta D, Daou BJ, Sukovich JR, et al. Transcranial MR-guided histotripsy system. IEEE Trans Ultrason, Ferroelect, Freq Control. 2021;68(9):2917–29.

[45]. Swietlik JF, Knott EA, Longo KC, Zlevor AM, Zhang X, Laeseke PF, et al. Histotripsy of subcutaneous fat in a live porcine model. CardioVasc Interv Radiol. 2023;46(1):120–7.

[46]. Vlaisavljevich E, Xu Z, Maxwell AD, Mancia L, Zhang X, Lin KW, et al. Effects of temperature on the histotripsy intrinsic threshold for cavitation. IEEE Trans Ultrason, Ferroelect, Freq Control. 2016;63(8):1064–77.

[47]. Lin KW, Duryea AP, Kim Y, Hall TL, Xu Z, Cain CA. Dual-beam histotripsy: A low-frequency pump enabling a high-frequency probe for precise lesion formation. IEEE Trans Ultrason, Ferroelect, Freq Control. 2014;61(2):325–40.

[48]. Vlaisavljevich E, Gerhardson T, Hall T, Xu Z. Effects of f-number on the histotripsy intrinsic threshold and cavitation bubble cloud behavior. Phys Med Biol. 2017;62(4):1269. [PubMed: 27995900]

[49]. Vlaisavljevich E, Lin K-W, Warnez MT, Singh R, Mancia L, Putnam AJ, et al. Effects of tissue stiffness, ultrasound frequency, and pressure on histotripsy-induced cavitation bubble behavior. Phys Med Biol. 2015;60(6):2271. [PubMed: 25715732]

[50]. Khokhlova T, Rosnitskiy P, Hunter C, Maxwell A, Kreider W, ter Haar G, et al. Dependence of inertial cavitation induced by high intensity focused ultrasound on transducer F-number and nonlinear waveform distortion. J Acoust Soc Am. 2018;144(3):1160–9. [PubMed: 30424663]

[51]. Rosnitskiy PB, Yuldashev PV, Sapozhnikov OA, Maxwell AD, Kreider W, Bailey MR, et al. Design of HIFU transducers for generating specified nonlinear ultrasound fields. IEEE Trans Ultrason, Ferroelect, Freq Control. 2017;64(2):374–90.

[52]. Bawiec CR, Rosnitskiy PB, Peek AT, Maxwell AD, Kreider W, Haar GRt, et al. Inertial cavitation behaviors induced by nonlinear focused ultrasound pulses. IEEE Trans Ultrason, Ferroelect, Freq Control. 2021;68(9):2884–95.

[53]. Wang T-Y, Xu Z, Hall TL, Fowlkes JB, Cain CA. An efficient treatment strategy for histotripsy by removing cavitation memory. Ultrasound Med Biol. 2012;38(5):753–66. [PubMed: 22402025]

[54]. Simon A, Edsall C, Vlaisavljevich E, editors. Effects of pulse repetition frequency on bubble cloud characteristics and ablation for single-cycle histotripsy. Final Program and Abstract Book of the 183rd meeting of the Acoustical Society of America; 2022; Nashville, TN, Dec. 5-9,.

[55]. Shi A, Xu Z, Lundt J, Tamaddoni HA, Worlikar T, Hall TL. Integrated histotripsy and bubble coalescence transducer for rapid tissue ablation. IEEE Trans Ultrason, Ferroelect, Freq Control. 2018;65(10):1822–31.

[56]. Maxwell A, Sapozhnikov O, Bailey M, Crum L, Xu Z, Fowlkes B, et al. Disintegration of tissue using high intensity focused ultrasound: Two approaches that utilize shock waves. Acoustics Today. 2012.

[57]. Maxwell AD, Owens G, Gurm HS, Ives K, Myers DD, Xu Z. Noninvasive treatment of deep venous thrombosis using pulsed ultrasound cavitation therapy (histotripsy) in a porcine model. J Vasc Interv Radiol. 2011;22(3):369–77. [PubMed: 21194969]

[58]. Vlaisavljevich E, Maxwell A, Warnez M, Johnsen E, Cain CA, Xu Z. Histotripsy-induced cavitation cloud initiation thresholds in tissues of different mechanical properties. IEEE Trans Ultrason, Ferroelect, Freq Control. 2014;61(2):341–52.

[59]. Kreider W, Maxwell AD, Khokhlova T, Simon JC, Khokhlova VA, Sapozhnikov O, et al. Rectified growth of histotripsy bubbles. Proc Meet Acoust. 2013;19(1):075035. [PubMed: 26413193]

[60]. Bader KB, Bollen V. The influence of gas diffusion on bubble persistence in shock-scattering histotripsy. J Acoust Soc Am. 2018;143(6):EL481–EL6. [PubMed: 29960422]

[61]. Park S, Maxwell AD, Owens GE, Gurm HS, Cain CA, Xu Z. Non-invasive embolus trap using histotripsy—an acoustic parameter study. Ultrasound Med Biol. 2013;39(4):611–9. [PubMed: 23415285]

[62]. Maxwell AD, Park S, Vaughan BL, Cain CA, Grotberg JB, Xu Z. Trapping of embolic particles in a vessel phantom by cavitation-enhanced acoustic streaming. Phys Med Biol. 2014;59(17):4927. [PubMed: 25109407]

[63]. Pahk KJ, Lee S, Gélat P, de Andrade MO, Saffari N. The interaction of shockwaves with a vapour bubble in boiling histotripsy: The shock scattering effect. Ultrason Sonochem. 2021;70:105312. [PubMed: 32866882]

[64]. Simon JC, Sapozhnikov OA, Wang Y-N, Khokhlova VA, Crum LA, Bailey MR. Investigation into the mechanisms of tissue atomization by high-intensity focused ultrasound. Ultrasound Med Biol. 2015;41(5):1372–85. [PubMed: 25662182]

[65]. Khokhlova TD, Monsky WL, Haider YA, Maxwell AD, Wang Y-N, Matula TJ. Histotripsy liquefaction of large hematomas. Ultrasound Med Biol. 2016;42(7):1491–8. [PubMed: 27126244]

[66]. Ponomarchuk EM, Hunter C, Song M, Khokhlova VA, Sapozhnikov OA, Yuldashev PV, et al. Mechanical damage thresholds for hematomas near gas-containing bodies in pulsed HIFU fields. Phys Med Biol. 2022;67(21):215007.

[67]. Rosnitskiy PB, Yuldashev PV, Khokhlova VA. Effect of the angular aperture of medical ultrasound transducers on the parameters of nonlinear ultrasound field with shocks at the focus. Acoust Phys. 2015;61(3):301–7.

[68]. Smallcomb M, Elliott J, Khandare S, Butt AA, Vidt ME, Simon JC. Focused ultrasound mechanical disruption of ex vivo rat tendon. IEEE Trans Ultrason, Ferroelect, Freq Control. 2021;68(9):2981–6.

[69]. Li Y, Hall TL, Xu Z, Cain CA. Enhanced shock scattering histotripsy with pseudomonopolar ultrasound pulses. IEEE Trans Ultrason, Ferroelect, Freq Control. 2019;66(7):1185–97.

[70]. Pahk KJ. Control of the dynamics of a boiling vapour bubble using pressure-modulated high intensity focused ultrasound without the shock scattering effect: A first proof-of-concept study. Ultrason Sonochem. 2021;77:105699. [PubMed: 34371476]

[71]. Pahk KJ, Heo J, Joung C, Pahk K. Noninvasive mechanical destruction of liver tissue and tissue decellularisation by pressure-modulated shockwave histotripsy. Frontiers in Immunology. 2023;14.

[72]. Thomas GPL, Khokhlova TD, Sapozhnikov OA, Khokhlova VA. Enhancement of boiling histotripsy by steering the focus axially during the pulse delivery. IEEE Trans Ultrason, Ferroelect, Freq Control. 2023;(In press).

[73]. Landry TG, Gannon J, Vlaisavljevich E, Mallay MG, Woodacre JK, Croul S, et al. Endoscopic coregistered ultrasound imaging and precision histotripsy: Initial in vivo evaluation. BME Frontiers. 2022;2022:ID 9794321.

[74]. Maxwell AD, Yuldashev PV, Kreider W, Khokhlova TD, Schade GR, Hall TL, et al. A prototype therapy system for transcutaneous application of boiling histotripsy. IEEE Trans Ultrason, Ferroelect, Freq Control. 2017;64(10):1542–57.

[75]. Edsall C, Ham E, Holmes H, Hall TL, Vlaisavljevich E. Effects of frequency on bubble-cloud behavior and ablation efficiency in intrinsic threshold histotripsy. Phys Med Biol. 2021;66(22):225009.

[76]. Bawiec CR, Khokhlova TD, Sapozhnikov OA, Rosnitskiy PB, Cunitz BW, Ghanem MA, et al. A prototype therapy system for boiling histotripsy in abdominal targets based on a 256-element spiral array. IEEE Trans Ultrason, Ferroelect, Freq Control. 2021;68(5):1496–510.

[77]. Ruger L, Yang E, Gannon J, Sheppard H, Coutermarsh-Ott S, Ziemlewicz TJ, et al. Mechanical high-intensity focused ultrasound (histotripsy) in dogs with spontaneously occurring soft tissue sarcomas. IEEE Trans Biomed Eng. 2023;70(3):768–79. [PubMed: 36006886]

[78]. Bollen V, Hendley SA, Paul JD, Maxwell AD, Haworth KJ, Holland CK, et al. In vitro thrombolytic efficacy of single- and five-cycle histotripsy pulses and rt-PA. Ultrasound Med Biol. 2020;46(2):336–49. [PubMed: 31785841]

[79]. Kim Y, Vlaisavljevich E, Owens GE, Allen SP, Cain CA, Xu Z. In vivo transcostal histotripsy therapy without aberration correction. Phys Med Biol. 2014;59(11):2553. [PubMed: 24785433]

[80]. Vlaisavljevich E, Kim Y, Allen S, Owens G, Pelletier S, Cain C, et al. Image-guided non-invasive ultrasound liver ablation using histotripsy: Feasibility study in an in vivo porcine model. Ultrasound Med Biol. 2013;39(8):1398–409. [PubMed: 23683406]

[81]. Matula TJ, Wang Y-N, Khokhlova T, Leotta DF, Kucewicz J, Brayman AA, et al. Treating porcine abscesses with histotripsy: A pilot study. Ultrasound Med Biol. 2021;47(3):603–19. [PubMed: 33250219]

[82]. Maxwell AD, Hsi RS, Bailey MR, Casale P, Lendvay TS. Noninvasive ureterocele puncture using pulsed focused ultrasound: An in vitro study. Journal of Endourology. 2013;28(3):342–6. [PubMed: 24171441]

[83]. Worlikar T, Mendiratta-Lala M, Vlaisavljevich E, Hubbard R, Shi J, Hall TL, et al. Effects of histotripsy on local tumor progression in an in vivo orthotopic rodent liver tumor model. BME Frontiers. 2020;9830304. [PubMed: 34327513]

[84]. Chevillet JR, Khokhlova TD, Giraldez MD, Schade GR, Starr F, Wang Y-N, et al. Release of cell-free microrna tumor biomarkers into the blood circulation with pulsed focused ultrasound: A noninvasive, anatomically localized, molecular liquid biopsy. Radiology. 2016;283(1):158–67. [PubMed: 27802108]

[85]. Schade GR, Wang Y-N, D'Andrea S, Hwang JH, Liles WC, Khokhlova TD. Boiling histotripsy ablation of renal cell carcinoma in the eker rat promotes a systemic inflammatory response. Ultrasound Med Biol. 2019;45(1):137–47. [PubMed: 30340920]

[86]. Khokhlova VA, Rosnitskiy PB, Yuldashev PV, Khokhlova TD, Sapozhnikov OA, Gavrilov LR, et al., editors. Design of a transrectal probe for boiling histotripsy ablation of prostate. Final Program and Abstract Book of the 18th International Symposium on Therapeutic Ultrasound; 2018; Nashville, TN (May 14 - 17, 2018).

[87]. Schade GR, Khokhlova TD, Hunter C, Kreider W, Rosnitskiy PB, Yuldashev PV, et al., editors. A preclinical transrectal boiling histotripsy system for prostate ablation. Abstract Book of the 34rd Annual Meeting of Engineering and Urology Society (EUS); 2019; Chicago, IL (May 5, 2019).

[88]. Schade GR, Khokhlova TD, Hunter C, Kreider W, Rosnitskiy PB, Yuldashev PV, et al., editors. A preclinical transrectal system for boiling histotripsy prostate ablation. Abstract Book of the 19th Internarional Symposium of ISTU; 2019; Barcelona, Spain (June 13-15, 2019).

[89]. Hall T, Cain C. A low cost compact 512 channel therapeutic ultrasound system for transcutaneous ultrasound surgery. AIP Conference Proceedings. 2006;829(1):445–9.

[90]. Hoogenboom M, Eikelenboom D, den Brok MH, Veltien A, Wassink M, Wesseling P, et al. In vivo MR guided boiling histotripsy in a mouse tumor model evaluated by mri and histopathology. NMR in Biomedicine. 2016;29(6):721–31. [PubMed: 27061290]

[91]. Karzova MM, Kreider W, Partanen A, Khokhlova TD, Sapozhnikov OA, Yuldashev PV, et al. Comparative characterization of nonlinear ultrasound fields generated by sonalleve v1 and v2 MR-HIFU systems. IEEE Trans Ultrason, Ferroelect, Freq Control. 2023:Advance online publication.

[92]. Hoogenboom M, van Amerongen MJ, Eikelenboom DC, Wassink M, den Brok MH, Hulsbergen-van de Kaa C, et al. Development of a high-field MR-guided HIFU setup for thermal and mechanical ablation methods in small animals. Journal of Therapeutic Ultrasound. 2015;3(1):14. [PubMed: 26269744]

[93]. Woodacre JK, Landry TG, Brown JA. Fabrication and characterization of a 5 mm × 5 mm aluminum lens-based histotripsy transducer. IEEE Trans Ultrason, Ferroelect, Freq Control. 2022;69(4):1442–51.

[94]. Woodacre JK, Landry TG, Brown JA. A low-cost miniature histotripsy transducer for precision tissue ablation. IEEE Trans Ultrason, Ferroelect, Freq Control. 2018;65(11):2131–40.

[95]. Mallay MG, Woodacre JK, Landry TG, Campbell NA, Brown JA. A dual-frequency lens-focused endoscopic histotripsy transducer. IEEE Trans Ultrason, Ferroelect, Freq Control. 2021;68(9):2906–16.

[96]. Mallay M, Greige J, Landry T, Campbell C, Woodacre J, Ibrahim M, et al., editors. Evaluation of piezoelectric ceramics for use in miniature histotripsy transducers. 2022 IEEE International Ultrasonics Symposium (IUS); 2022 10-13 Oct. 2022.

[97]. Uchino K. Ceramic actuators: Principles and applications. MRS Bulletin. 1993;18(4):42–8.

[98]. N-Nagy FL, Joyce GC. Solid state control elements operating on physical principles. In: Mason WP, Thurston RN, editors. Physical acoustics. 9. NY: Academic Press; 1972. p. 131.

[99]. Knott EA, Swietlik JF, Longo KC, Watson RF, Green CM, Abel EJ, et al. Robotically-assisted sonic therapy for renal ablation in a live porcine model: Initial preclinical results. J Vasc Interv Radiol. 2019;30(8):1293–302. [PubMed: 31130365]

[100]. Vidal-Jove J, Serres X, Vlaisavljevich E, Cannata J, Duryea A, Miller R, et al. First-in-man histotripsy of hepatic tumors: The theresa trial, a feasibility study. Int J Hyperthermia. 2022;39(1):1115–23. [PubMed: 36002243]

[101]. Hendricks-Wenger A, Arnold L, Gannon J, Simon A, Singh N, Sheppard H, et al. Histotripsy ablation in preclinical animal models of cancer and spontaneous tumors in veterinary patients: A review. IEEE Trans Ultrason, Ferroelect, Freq Control. 2022;69(1):5–26.

[102]. Eranki A, Srinivasan P, Ries M, Kim A, Lazarski CA, Rossi CT, et al. High-intensity focused ultrasound (HIFU) triggers immune sensitization of refractory murine neuroblastoma to checkpoint inhibitor therapy. Clinical Cancer Research. 2020;26(5):1152–61. [PubMed: 31615935]

[103]. Qu S, Worlikar T, Felsted AE, Ganguly A, Beems MV, Hubbard R, et al. Non-thermal histotripsy tumor ablation promotes abscopal immune responses that enhance cancer immunotherapy. Journal for ImmunoTherapy of Cancer. 2020;8(1):e000200. [PubMed: 31940590]

[104]. Singh MP, Sethuraman SN, Miller C, Malayer J, Ranjan A. Boiling histotripsy and in-situ cd40 stimulation improve the checkpoint blockade therapy of poorly immunogenic tumors. Theranostics. 2021;11(2):540–54. [PubMed: 33391491]

[105]. van den Bijgaart RJE, Mekers VE, Schuurmans F, Raaijmakers TK, Wassink M, Veltien A, et al. Mechanical high-intensity focused ultrasound creates unique tumor debris enhancing dendritic cell-induced t cell activation. Frontiers in Immunology. 2022;13.

[106]. Schuster TG, Wei JT, Hendlin K, Jahnke R, Roberts WW. Histotripsy treatment of benign prostatic enlargement using the vortx rx system: Initial human safety and efficacy outcomes. Urology. 2018;114:184–7. [PubMed: 29330000]

[107]. Roberts W,W, Teofilovic D, Jahnke R,C, Patri J, Risdahl J,M, Bertolina J,A Histotripsy of the prostate using a commercial system in a canine model. J Urol. 2014;191(3):860–5. [PubMed: 24012583]

[108]. Pichardo S, Gelet A, Curiel L, Chesnais S, Chapelon JY. New integrated imaging high intensity focused ultrasound probe for transrectal prostate cancer treatment. Ultrasound Med Biol. 2008;34(7):1105–16. [PubMed: 18258351]

[109]. Sekar RR, Singh Z, Khokhlova TD, Peek AT, Wang Y-N, Son H, et al., editors. Initial preclinical results of a prototype transrectal histotripsy device for prostate cancer ablation. Final Program and Abstract Book of the 19th International Symposium of ISTU; 2021; Gyeongju, Korea (June 6-9, 2021).

[110]. Lee JY, Kim K, Hwang SI, Lee M, Son K, Kim D, et al. Efficacy and safety of transvaginal high-intensity focused ultrasound therapy in women with symptomatic uterine leiomyomas: A clinical trial. European Journal of Obstetrics & Gynecology and Reproductive Biology. 2021;256:302–7. [PubMed: 33259999]

[111]. Li T, Khokhlova T, Maloney E, Wang Y-N, D'Andrea S, Starr F, et al. Endoscopic high-intensity focused us: Technical aspects and studies in an in vivo porcine model (with video). Gastrointestinal Endoscopy. 2015;81(5):1243–50. [PubMed: 25759124]

[112]. Pioche M, Lafon C, Constanciel E, Vignot A, Birer A, Gincul R, et al. High-intensity focused ultrasound liver destruction through the gastric wall under endoscopic ultrasound control: First experience in living pigs. Endoscopy. 2012;44(S 02):E376–E7. [PubMed: 23012031]

[113]. Canney MS, Chavrier F, Tsysar S, Chapelon J-Y, Lafon C, Carpentier A. A multi-element interstitial ultrasound applicator for the thermal therapy of brain tumors. J Acoust Soc Am. 2013;134(2):1647–55. [PubMed: 23927205]

[114]. Nanda Kumar Y, Singh Z, Wang Y-N, Schade GR, Kreider W, Bruce M, et al. Development of tough hydrogel phantoms to mimic fibrous tissue for focused ultrasound therapies. Ultrasound Med Biol. 2022;48(9):1762–77. [PubMed: 35697582]

[115]. Khokhlova VA, Rosnitskiy PB, Tsysar SA, Buravkov SV, Ponomarchuk EM, Sapozhnikov OA, et al. Initial assessment of boiling histotripsy for mechanical ablation of ex vivo human prostate tissue. Ultrasound Med Biol. 2023;49(1):62–71. [PubMed: 36207225]

[116]. Simon A, Robinson F, Anzivino A, Boyer M, Hendricks-Wenger A, Guilliams D, et al. Histotripsy for the treatment of uterine leiomyomas: A feasibility study in ex vivo uterine fibroids. Ultrasound Med Biol. 2022;48(8):1652–62. [PubMed: 35641394]

[117]. Zhang X, Owens GE, Cain CA, Gurm HS, Macoskey J, Xu Z. Histotripsy thrombolysis on retracted clots. Ultrasound Med Biol. 2016;42(8):1903–18. [PubMed: 27166017]

[118]. Bader KB, Haworth KJ, Shekhar H, Maxwell AD, Peng T, McPherson DD, et al. Efficacy of histotripsy combined with rt-PA in vitro. Phys Med Biol. 2016;61(14):5253. [PubMed: 27353199]

[119]. Hendley SA, Paul JD, Maxwell AD, Haworth KJ, Holland CK, Bader KB. Clot degradation under the action of histotripsy bubble activity and a lytic drug. IEEE Trans Ultrason, Ferroelect, Freq Control. 2021;68(9):2942–52.

[120]. Prada F, Kalani MYS, Yagmurlu K, Norat P, Del Bene M, DiMeco F, et al. Applications of focused ultrasound in cerebrovascular diseases and brain tumors. Neurotherapeutics. 2019;16(1):67–87. [PubMed: 30406382]

[121]. Gerhardson T, Sukovich JR, Chaudhary N, Chenevert TL, Ives K, Hall TL, et al. Histotripsy clot liquefaction in a porcine intracerebral hemorrhage model. Neurosurgery. 2020;86(3).

[122]. Lu N, Gupta D, Daou BJ, Fox A, Choi D, Sukovich JR, et al. Transcranial magnetic resonance-guided histotripsy for brain surgery: Pre-clinical investigation. Ultrasound Med Biol. 2022;48(1):98–110. [PubMed: 34615611]

[123]. Lu N, Hall TL, Sukovich JR, Choi SW, Snell J, McDannold N, et al. Two-step aberration correction: Application to transcranial histotripsy. Phys Med Biol. 2022;67(12):125009.

[124]. Macoskey JJ, Hall TL, Sukovich JR, Choi SW, Ives K, Johnsen E, et al. Soft-tissue aberration correction for histotripsy. IEEE Trans Ultrason, Ferroelect, Freq Control. 2018;65(11):2073–85.

[125]. Sukovich JR, Macoskey JJ, Lundt JE, Gerhardson TI, Hall TL, Xu Z. Real-time transcranial histotripsy treatment localization and mapping using acoustic cavitation emission feedback. IEEE Trans Ultrason, Ferroelect, Freq Control. 2020;67(6):1178–91.

[126]. Allen SP, Hall TL, Cain CA, Hernandez-Garcia L. Controlling cavitation-based image contrast in focused ultrasound histotripsy surgery. Magn Reson Med. 2015;73(1):204–13. [PubMed: 24469922]

[127]. Rosnitskiy PB, Yuldashev PV, Sapozhnikov OA, Gavrilov LR, Khokhlova VA. Simulation of nonlinear trans-skull focusing and formation of shocks in brain using a fully populated ultrasound array with aberration correction. J Acoust Soc Am. 2019;146(3):1786–98. [PubMed: 31590513]

[128]. Goudot G, Khider L, Del Giudice C, Mirault T, Galloula A, Bruneval P, et al. Non-invasive recanalization of deep venous thrombosis by high frequency ultrasound in a swine model with follow-up. J Thromb Haemost. 2020;18(11):2889–98. [PubMed: 32741128]

[129]. Owens GE, Miller RM, Ensing G, Ives K, Gordon D, Ludomirsky A, et al. Therapeutic ultrasound to noninvasively create intracardiac communications in an intact animal model. Catheter Cardiovasc Interv. 2011;77(4):580–8. [PubMed: 20853366]

[130]. Erriu M, Blus C, Szmukler-Moncler S, Buogo S, Levi R, Barbato G, et al. Microbial biofilm modulation by ultrasound: Current concepts and controversies. Ultrason Sonochem. 2014;21(1):15–22. [PubMed: 23751458]

[131]. Bigelow TA, Thomas CL, Wu H, Itani KMF. Impact of high-intensity ultrasound on strength of surgical mesh when treating biofilm infections. IEEE Trans Ultrason, Ferroelect, Freq Control. 2019;66(1):38–44.

[132]. Childers C, Edsall C, Gannon J, Whittington AR, Muelenaer AA, Rao J, et al. Focused ultrasound biofilm ablation: Investigation of histotripsy for the treatment of catheter-associated urinary tract infections (cautis). IEEE Trans Ultrason, Ferroelect, Freq Control. 2021;68(9):2965–80.

[133]. Brayman AA, MacConaghy BE, Wang Y-N, Chan KT, Monsky WL, Chernikov VP, et al. Inactivation of planktonic escherichia coli by focused 1-mhz ultrasound pulses with shocks: Efficacy and kinetics upon volume scale-up. Ultrasound Med Biol. 2018;44(9):1996–2008. [PubMed: 29941214]

[134]. Hinkelman LM, Mast TD, Metlay LA, Waag RC. The effect of abdominal wall morphology on ultrasonic pulse distortion. Part i. Measurements. J Acoust Soc Am. 1998;104(6):3635–49. [PubMed: 9857521]

[135]. Ritchie R, Collin J, Coussios C, Leslie T. Attenuation and de-focusing during high-intensity focused ultrasound therapy through peri-nephric fat. Ultrasound Med Biol. 2013;39(10):1785–93. [PubMed: 23932273]

[136]. Thomas GPL, Khokhlova TD, Bawiec CR, Peek AT, Sapozhnikov OA, O'Donnell M, et al. Phase-aberration correction for HIFU therapy using a multielement array and backscattering of nonlinear pulses. IEEE Trans Ultrason, Ferroelect, Freq Control. 2021;68(4):1040–50.

[137]. Thomas GPL, Khokhlova TD, Sapozhnikov OA, Wang YN, Totten SI, Khokhlova VA. In vivo aberration correction for transcutaneous HIFU therapy using a multielement array. IEEE Trans Ultrason, Ferroelect, Freq Control. 2022;69(10):2955–64.

[138]. Yeats E, Gupta D, Xu Z, Hall TL. Effects of phase aberration on transabdominal focusing for a large aperture, low f-number histotripsy transducer. Phys Med Biol. 2022;67(15):155004.

[139]. Yeats E, Lu N, Sukovich JR, Xu Z, Hall TL. Soft tissue aberration correction for histotripsy using acoustic emissions from cavitation cloud nucleation and collapse. Ultrasound Med Biol. 2023;49(5):1182–93. [PubMed: 36759271]

[140]. Pernot M, Montaldo G, Tanter M, Fink M. "Ultrasonic stars" for time-reversal focusing using induced cavitation bubbles. Applied Physics Letters. 2006;88(3):034102.

[141]. Elliott J, Simon JC. Histotripsy bubble dynamics in elastic, anisotropic tissue-mimicking phantoms. Ultrasound Med Biol. 2023;49(3):853–65. [PubMed: 36577567]

[142]. Wang TY, Hall TL, Xu Z, Fowlkes JB, Cain CA. Imaging feedback of histotripsy treatments using ultrasound shear wave elastography. IEEE Trans Ultrason, Ferroelect, Freq Control. 2012;59(6):1167–81.

[143]. Miller RM, Zhang X, Maxwell AD, Cain CA, Xu Z. Bubble-induced color doppler feedback for histotripsy tissue fractionation. IEEE Trans Ultrason, Ferroelect, Freq Control. 2016;63(3):408–19.

[144]. Anthony GJ, Bollen V, Hendley S, Antic T, Sammet S, Bader KB. Assessment of histotripsy-induced liquefaction with diagnostic ultrasound and magnetic resonance imaging in vitro and ex vivo. Phys Med Biol. 2019;64(9):095023. [PubMed: 30921780]

[145]. Kutlu AZ, Laeseke PF, Zeighami Salimabad M, Minesinger GM, Periyasamy S, Pieper AA, et al. A multimodal phantom for visualization and assessment of histotripsy treatments on ultrasound and x-ray imaging. Ultrasound Med Biol. 2023;49(6):1401–7. [PubMed: 36878828]

[146]. Wagner MG, Periyasamy S, Kutlu AZ, Pieper AA, Swietlik JF, Ziemlewicz TJ, et al. An x-ray c-arm guided automatic targeting system for histotripsy. IEEE Trans Biomed Eng. 2023;70(2):592–602. [PubMed: 35984807]

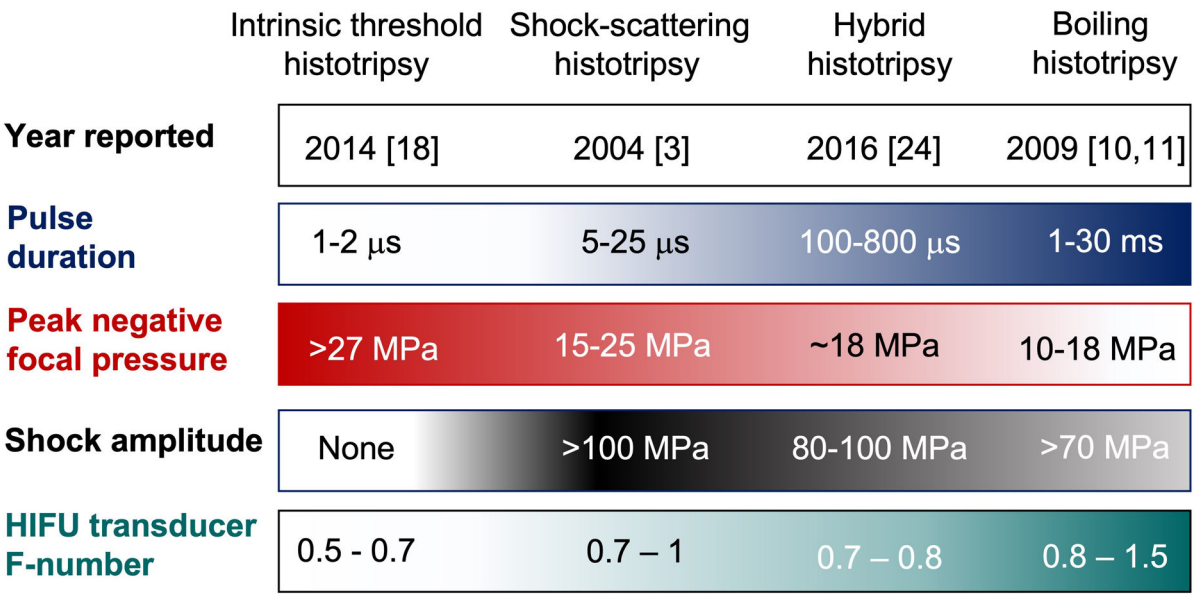

Figure 1.

Histotripsy techniques and associated representative acoustic parameters. The year refers to the time when each technique was first reported in literature, but not yet necessarily termed the way it is currently known. HIFU transducer *F*-number is the ratio of its radius of curvature (focal length) to the aperture diameter. The first two types are typically used at frequencies less than 1 MHz, and last two at frequencies higher than 1 MHz.

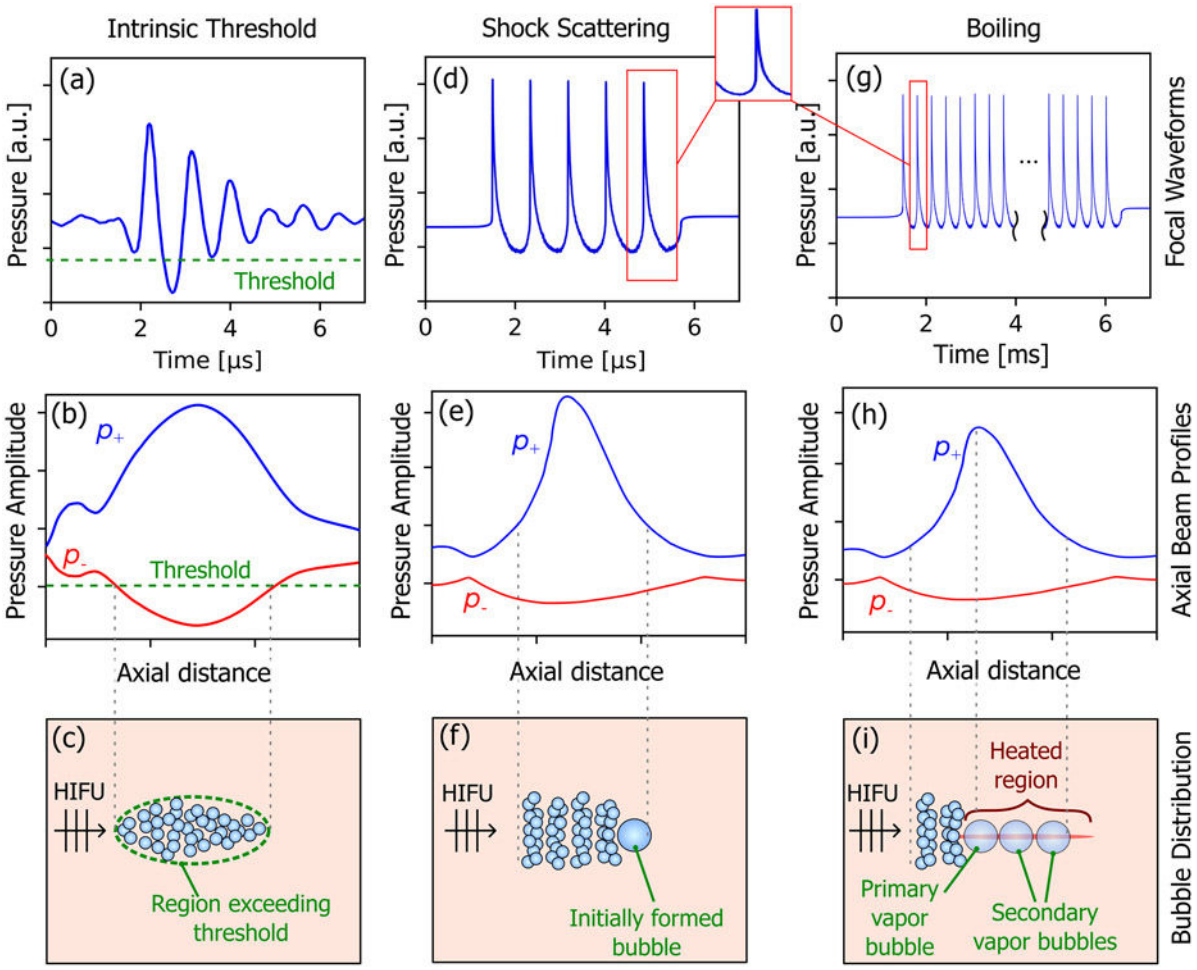

Figure 2.

Comparison of typical focal pressure waveforms (top row), free-field axial beam profiles (middle row), and resulting bubble distributions for intrinsic threshold histotripsy (left column), shock scattering histotripsy (middle column), and boiling histotripsy (right column). For intrinsic threshold histotripsy, a short pulse is generated with a single dominant tensile pressure cycle exceeding the intrinsic threshold. Both shock scattering histotripsy and boiling histotripsy utilize focal pressure waveforms containing high amplitude shocks at the focus, and a bubble cloud forms due to interaction of the shocks with an initially formed (incidental) bubble. In shock scattering histotripsy, the initial bubble forms in response to one or more tensile phases of the excitation pressure, while shock-induced heating causes the primary vapor bubble to form in boiling histotripsy. Note that the bubbles have not been drawn to scale.

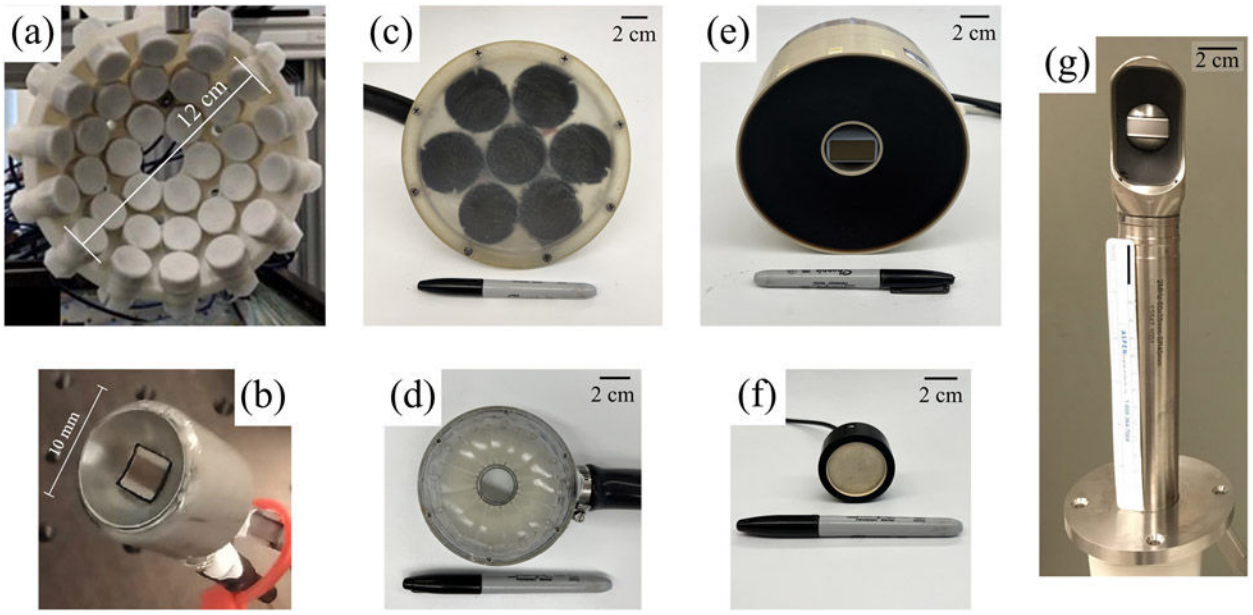

Figure 3.

Examples of transducers used for intrinsic threshold histotripsy (a, b), shock-scattering histotripsy (c, d), and boiling histotripsy (e, f, g). Subfigures (a) and (b) are modified from [75] and [73], respectively, and are licensed under a Creative Commons Attribution License (CC BY 4.0).